Distribution Agreement

In presenting this thesis as a partial fulfillment of the requirements for a degree from Emory University, I hereby grant to Emory University and its agents the non-exclusive license to archive, make accessible, and display my thesis in whole or in part in all forms of media, now or hereafter now, including display on the World Wide Web. I understand that I may select some access restrictions as part of the online submission of this thesis. I retain all ownership rights to the copyright of the thesis. I also retain the right to use in future works (such as articles or books) all or part of this thesis.

Ross Greenberg April 7, 2020

The population and evolutionary dynamics of competition between *Pseudomonas aeruginosa* and *Staphylococcus aureus*

by

Ross Greenberg

Bruce Levin, Ph.D.
Adviser

Biology

Bruce Levin, Ph.D.

Adviser

Joanna Goldberg, Ph.D.

Committee Member

Nicole Vega, Ph.D.

Committee Member

Marvin Whiteley, Ph.D.

Committee Member

2020

The population and evolutionary dynamics of competition between *Pseudomonas aeruginosa* and *Staphylococcus aureus*

By

Ross Greenberg

Bruce Levin, Ph.D.

Adviser

An abstract of
a thesis submitted to the Faculty of Emory College of Arts and Sciences
of Emory University in partial fulfillment
of the requirements of the degree of
Bachelor of Science with Honors

Biology

2020

Abstract

The population and evolutionary dynamics of competition between *Pseudomonas aeruginosa* and *Staphylococcus aureus*

By Ross Greenberg

Pseudomonas aeruginosa and *Staphylococcus aureus* regularly co-infect the lungs of cystic fibrosis (CF) patients. However, *P. aeruginosa* either kills or inhibits the growth of *S. aureus* when co-cultured *in vitro*. The current consensus is that the *P. aeruginosa* PQS quorum sensing system, specifically 4-hydroxy-2-heptoquinoline-N-oxide (HQNO), is responsible for this antagonism. Although much is known the role of HQNO in this antagonism at the molecular and cellular level, there remain fundamental unanswered ecological and evolutionary questions about the antagonistic interaction between these Gram-negative and Gram-positive bacteria. The goal of this jointly theoretical and *in vitro* experimental study is to address and answer the following questions: 1) Are there population interactions, other than those mediated by HQNO, that contribute to this antagonism? 2) To what extent does antagonism by *P. aeruginosa* contribute to the ecology of *S. aureus*? 3) Is the mechanism of this antagonism purely extracellular, or does it require cell-to-cell contact? 4) What are the selective forces responsible for the evolution of this antagonistic phenomenon? Addressing these questions will provide a framework to better understand the ecology the CF lung infections. Using a combination of mathematical modelling and *in vitro* experiments with *P. aeruginosa* and *S. aureus,* we address and provide answers to these questions. We present evidence for frequency and density dependence of *P. aeruginosa* antagonism towards *S. aureus*. Simple resource competition, extracellular allelopathy, and contact-dependent inhibition alone cannot explain the observed dynamics. *S. aureus* has a growth disadvantage when cultured in the presence of sonicated *P. aeruginosa* supernatant, implying the existence of an extracellular layer to the mechanism. Nevertheless, the presence of *P. aeruginosa* cell-free extract does alter the change in growth fold of *S. aureus*. A significant decline in *S. aureus* population is, however, observed when it is cultured in the presence of non-replicating *P. aeruginosa* culture, implying that the killing itself is either dependent of cell-cell contact or induction by an *S. aureus* exoproduct. Variations on models wherein *P. aeruginosa* lyses *S. aureus* and uses resources liberated from the ruptured cells, or in which *P. aeruginosa* utilizes passively released *S. aureus* exoproducts as a resource, best reflect the observed population dynamics and antagonistic phenomena.

The population and evolutionary dynamics of competition between *Pseudomonas aeruginosa* and *Staphylococcus aureus*

By

Ross Greenberg

Bruce Levin, Ph.D.

Adviser

A thesis submitted to the Faculty of Emory College of Arts and Sciences
of Emory University in partial fulfillment
of the requirements of the degree of
Bachelor of Science with Honors

Biology

2020

Acknowledgements

First, I would like to thank the members of the *Ec*LF group for assisting me with this project for the past year: Waqas, for teaching me how to conduct experiments and assisting me with obtaining the microscopy images; Ingrid for her help with questions regarding lab safety and experimental protocols; Brandon and Adithi for discussing ideas with me; Meloney and Esther for not only discussing science, but also for making always making sure there were enough plates to make this project possible; last, but certainly not least, Dr. Levin, for igniting an insatiable curiosity for gaining knowledge through the scientific method.

I would also like to thank all members of my committee for their guidance and flexibility throughout this entire process. I am grateful for Drs. Nic Vega and Marvin Whiteley allowing me to use their microscopes, and for Drs. Goldberg and Whiteley providing the strains used throughout this study. This project truly would not be possible without your help.

Finally, I would like to thank my parents and my brothers for their continuous support.

This research was funded by an NIH Grant, GM091875-17 and Emory University.

Table of Contents

Table of Contents (Continued)

INTRODUCTION

Background

An unyielding cough and persistent bacterial infection are two of the many challenges that cystic fibrosis (CF) patients must endure [1]. The morbidity and mortality of CF patients can to a large extent be attributed to bacterial infections. Two of the most common pathogens occurring in the CF lung are *Staphylococcus aureus* and *Pseudomonas aeruginosa* [2].

A typical natural history for CF lung infection is that patients are first infected by the opportunistic *S. aureus,* and then *P. aeruginosa* eventually establishes itself and outcompetes the *S. aureus* [1-4]. However, in some instances, *P. aeruginosa* and *S. aureus* can stably co-infect the lung. Co-infection is often associated with increased pathogenicity and poorer patient outcomes, including antibiotic treatment failure [5, 6].

It is well established that *P. aeruginosa* inhibits the growth of, or kills, *S. aureus in vitro*, and the mechanism of this inhibition has been the subject of numerous recent publications. The most established culprit for *P. aeruginosa* inhibition of *S. aureus* is the PQS (Pseudomonas Quinolone Signal) quorum sensing pathway present in *P. aeruginosa*, more specifically the compound 4-hydroxy-2-heptoquinoline-N-oxide (HQNO) [2, 6-8]. Alternative functions for quorum sensing molecules—such as iron sequestration, antimicrobial action, and alteration of membrane dynamics—have identified in many other instances [9].

HQNO is an electron transport chain (ETC) inhibitor of cytochrome b, which leads to decreased ATP production [6]. Filkins et al., 2015 provides further evidence for the ETC inhibition mechanism by showing that *S. aureus* shifts to fermentative metabolism when cultured in the presence of *P. aeruginosa* cell-free extracts. This eradication of ETC activity and shift towards fermentative metabolism caused by HQNO facilitates the selection of *S. aureus* small colony variants (SCV) [8]. Since SCV contain mutations that inhibit ETC function, they are better equipped to survive an ETC inhibitor like HQNO. *S. aureus* SCV are clinically relevant, as they are widely present in cystic fibrosis (CF) patient sputum and are resistant to a wide range of antibiotics, specifically aminoglycosides [8, 10].

Iron scavenging has been demonstrated as one driving force for *P. aeruginosa* inhibition of *S. aureus*. In an *in vivo* mouse model, wild-type *P. aeruginosa* PA14 downregulates the production of the iron-scavenging molecule (siderophore) pyoverdine in the presence of *S. aureus*, implying that PA14 senses higher iron levels in the presence of *S. aureus* [11]. This study also found that, the *P. aeruginosa* induction of *S. aureus* lysis is likely a necessary step for *P. aeruginosa* to maximally utilize the iron stores derived from *S. aureus* [11]. This lysis occurs late in the growth cycle, around the onset of *P. aeruginosa* stationary phase, yet is activated sooner when the two species are cultured in the presence of CF sputum [12]. The authors of that study attributed this changed dynamic to an earlier induction of stationary phase in *P. aeruginosa* [12].

The connection between the PQS quorum sensing system and iron scavenging is that the PQS molecule has been found to induce the production of the siderophores pyoverdine and pyochelin, while simultaneously sequestering iron to increase the likelihood of siderophore binding [13]. Further, a decreased concentration of iron in the growth media leads to increased inhibition of *S. aureus* by *P. aeruginosa* [14]. Taken together, it is evident that extracellular products, specifically in quorum sensing and iron acquisition pathways, mediate the *P. aeruginosa* inhibition, or killing, of *S. aureus*.

Virtually all studies of the *P. aeruginosa-S. aureus* systems focus on the physiological, molecular and genetic mechanisms responsible for the growth inhibition and killing of *S. aureus* by *P. aeruginosa*. However, relatively little consideration has been given to the ecological consequences and evolution of this antagonistic interaction. Fundamental questions remain unanswered, or nearly so: 1) What mechanisms at the population level, both including and beyond HQNO, contribute to the observed antagonism? 2) What are the effects of this antagonistic interaction on the ecology of *P. aeruginosa* and *S. aureus*? 3) Is the mechanism of this antagonistic interaction purely extracellular, (i.e. allelopathy), or does it require physical contact between *P. aeruginosa* and *S. aureus*? 4) What are the selective forces responsible for the evolution of this antagonistic interaction?

Cell Contact-Dependent Inhibition (CDI): An Important Caveat

Implicit in the above hypothesis about the role of HQNO is that the antagonism is solely mediated by extracellular processes, allelopathy, and that cell-cell contact does not play a role in the inhibitory interaction. However, this presupposition might not be true. A recent study featured time-lapse videos of *P. aeruginosa* and *S. aureus* cells interacting on two-dimensional surfaces. These films demonstrated that in the presence of *S. aureus*, individual *P. aeruginosa* cells break away from multicellular colony structures to surround and invade local *S. aureus* colonies [15]. The implications of this finding are: i) that *P. aeruginosa* can somehow sense the presence of *S. aureus*, and ii) that direct cell-cell contact may contribute to the inhibition of *S. aureus*. The presence of *S. aureus* influencing *P. aeruginosa* metabolism was also noted in Mashburn et al., 2005, with the presence of *S. aureus* increasing the growth yield of *P. aeruginosa.*

Research Strategy

The current study addresses and answers questions about the population-based mechanisms responsible for antagonistic interaction between *Pseudomonas aeruginosa* and *Staphylococcus aureus* with a combination of mathematical modeling and *in vitro* experiments with these bacteria. We separately consider the bacteria maintained in an unstructured environment—where all cells have equal access to each other, resources, toxins and wastes—and a physically structured environment where the bacteria exist as colonies. For the former investigation, Part I, we use mass action, ordinary differential equation (ODE) models, and experiments in well-agitated liquid culture to elucidate the relative roles of resource competition, antagonistic cell-cell interactions and extracellular allelopathy to the population dynamics of mixed cultures of *P. aeruginosa* and *S. aureus.* To address the inconvenient reality that the natural habitations of bacteria are physically structured, in Part II we perform these competition experiments with the bacteria interacting as colonies on surfaces.

Through our experiments in unstructured liquid culture, we demonstrate that competition for a shared resource plays little role in antagonistic interactions between *P. aeruginosa* and *S. aureus*, and that the antagonism operates via both cell-cell mediated processes and the release of extracellular allelopathic agents. One limitation of the methods used in the present study is that

CDI and extracellular allelopathy cannot be distinguished solely based on changes in the populations over time. It must also be noted that these two mechanisms are not mutually exclusive.

The present study also addresses the evolution of this antagonistic process in between *P. aeruginosa* and *S. aureus*. In resource-limited, mass action simulations of CDI and extracellular allelopathy systems that consist of two otherwise identical populations that only differ in the ability to perpetrate antagonism or be sensitive to that antagonism, the perpetrator cannot increase in frequency if initially rare in the population. This phenomenon is hypothesized to occur as a direct consequence of the mass action assumption: That is, if the sensitive population is present at a higher frequency, it is more likely to encounter the common resource and eventually exhaust that resource. Assuming that the perpetuation of antagonism, by extracellular or contact-dependent means, is resource-dependent, the lower concentration of resource available to a rare perpetuating population limits the amount of inhibition that can occur. In sum, one would hypothesize that perpetuating antagonism would provide no advantage to rare populations, and over time these genes are expected to be lost due to natural selection. However, the present study directly contradicts this hypothesis. *P. aeruginosa*, the "perpetrator", increases in frequency when initially rare, and eventually overtakes the population.

Based on this observation, we hypothesize that the antagonistic interaction likely operates via a mechanism that involves the conversion of *S. aureus* into a resource that can only be utilized by *P. aeruginosa.* We arrived to this *S. aureus*-derived resource hypothesis is based on earlier research, including Mashburn et al., 2005, which found evidence that *P. aeruginosa* lyses *S. aureus* to use it as an iron source. It is also consistent with studies that have demonstrated the ability of *P. aeruginosa* to grow on, and increase antimicrobial activity in the presence of, *N*-acetylglucosamine (GlcNAc) derived from the peptidoglycan walls of the gram-positive *S. aureus* cells. From our competition experiments of the two species on two-dimensional surfaces, we found evidence for this *S. aureus*-derived resource hypothesis, specifically the GlcNAc-based mechanism, and evidence against simple extracellular allelopathy.

It is critical to this hypothesis that the resource derived from *S. aureus* can only be used *P. aeruginosa*, for if it were available for consumption by both species, *P. aeruginosa* would not be able to increase in frequency if rare, due to the same logic described for the standard theory.

With this change, *P. aeruginosa* can compensate for its lack of access to the common resource by utilizing the resource derived from *S. aureus*. *P. aeruginosa* gaining the ability to utilize a new resource provides a potential explanation for the evolution of antagonism towards *S. aureus*.

MATERIALS AND METHODS

Bacteria

Wild-type (WT) *Pseudomonas aeruginosa* PAO1 and *Staphylococcus aureus* JE2 USA300 (SaJE2) were provided by Dr. Joanna B. Goldberg (Emory University). *S. aureus* JE2 is a plasmid-cured strain that was generated as part of the Nebraska Transposon Mutant library from a skin and soft tissue MRSA sample, obtained at the Los Angeles County Jail [16]. Dr. Marvin Whiteley (Georgia Institute of Technology/Emory University) provided GFP-labelled *P. aeruginosa* PAO1 (pCM29) with a transposon insertion in the *pqsL* gene. *pqsL* is a part of the PQS quorum sensing system, and its product synthesizes the immediate precursor to HQNO, 2-hydroxylaminobenzoylacetate (2-HABA) [17]. Dr. Whiteley also provided GFP and Dsred strains of PAO1 WT (pCM29) and *S. aureus* JE2 (pHC48), respectively.

Culture Media and Methods

Lysogeny Broth (LB) (244620, Difco™): Complex media that supports growth of both *P. aeruginosa* and *S. aureus*

Mannitol Salt Broth, Phenol Red (MSB) (Sigma-Aldrich®, BCBZ8813): Media for the selection and differentiation of *S. aureus*

Hard Agar Plates and Soft Agar Matrices: “Hard agar” mixtures for each given growth media were prepared by adding 1.5% agar by volume, and “soft agar” mixtures contained 0.6% agar by volume.

Estimating Bacterial Densities

To estimate the bacterial density (CFU/mL) of single-species samples, the cultures were serially diluted in 0.85% saline and spread on LB hard agar plates (1.5% agar). For *P.aeruginosa*/*S. aureus* mixed samples, the average density was measured by serially diluting the cultures in saline and spreading on LB hard agar plates and Mannitol Salt Agar (MSA) plates. *P. aeruginosa* and *S. aureus* can be distinguished on LB plates based on colony morphology, so LB plates were used to estimate *P. aeruginosa* density. *S. aureus* densities were estimated from the MSA plates. In addition, the PAO1 WT and *pqsL* strains have distinct morphologies on LB plates, and their densities can be obtained from the same plate. Cell densities were estimated by multiplying the colony counts by the dilution factor.

Growth Rates and Lag Times

Pure cultures of each strain were prepared and sampled after overnight incubation. 300 µL of 1/10,000 dilution, in LB, was loaded directly into to a Honeycomb® plate, for a total of ten replicates of each species. The Honeycomb® plate was placed into a BioScreen C ™ MBR.

Cultures were kept at 37˚ C. The optical density at 600 nm (OD_{600}) was taken every 5 minutes for 24 hours. Lag times were estimated as mean amount of time for the cultures to reach an OD_{600} of 0.02. Maximum growth rates and lag times were calculated using a custom R software package.

Statistical Tests

Statistical tests were performed using GraphPad® QuickCalcs. A confidence level (α) of 0.05 was used.

RESULTS

I. Competition and Antagonistic Interactions in Well-Mixed Liquid Culture

We open this consideration of the population and evolutionary dynamics of the antagonism between *P. aeruginosa* and *S. aureus* with the most common way bacterial competition is studied: in well-agitated liquid culture. The theoretical equivalent of this experimental system is the mass action model. The conditions described constitute an effectively dimensionless habitat, in which all individuals have equal access to each other, resources and allelopathic agents.

The First-Order Models and Predicted Dynamics: The three models used in the first part of this theoretical consideration are depicted in Figure 1. Although these models differ in the form of the interaction, in each case, the growth rate of the bacteria is determined by the following monotonic increasing function of the limiting resource concentration:

$$\psi(R) = v_i \frac{R}{(R + k_i)}$$

where R is the concentration of the limiting resource (μg/mL), v_i is the maximum growth rate of the i population (hr^{-1}), and k_i (μg) is the Monod constant. The Monod constant is defined as the resource concentration where the growth rate of the bacteria is half its maximum rate ($v_i/2$).

Resource Competition (Eq. 1-4, Fig. 1A): In this model, *P. aeruginosa* and *S. aureus* interact solely by their consumption of the common resource (R). Under these conditions, the rates of change in the densities of the competing *P. aeruginosa* (Pa) and *S. aureus* (Sa), in batch culture, are given by, N_{Pa} and N_{Sa}. The conversion efficiencies of the two species (e_{Pa} and e_{Sa}; units = μg/cell) are defined as the amount of the resource needed to produce a new cell [18]. The definitions of the parameters and variables in this model, and those that follow, are presented in Table 1 along with the values of the parameters used for the numerical solutions.

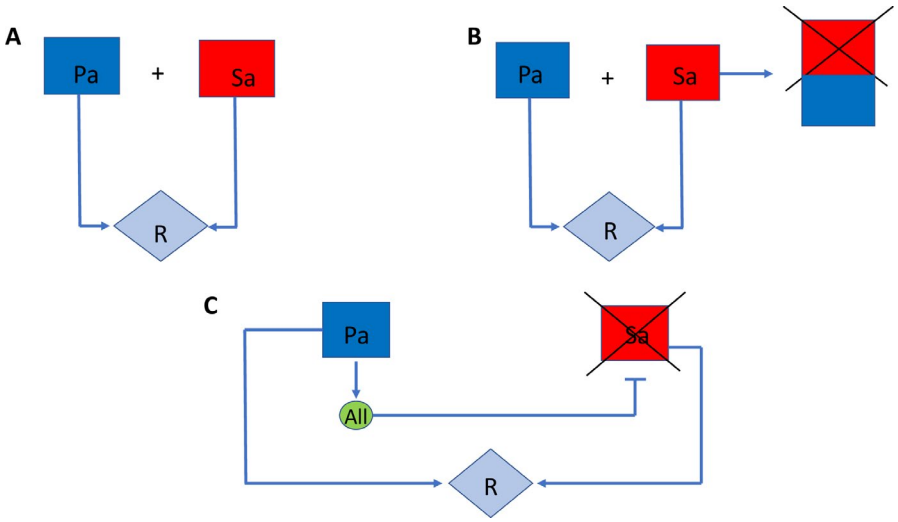

Figure 1: **Schematic diagrams of the basic theoretical models** In a simple resource competition model, *P. aeruginosa* (Pa) and *S. aureus* (Sa) compete for a common resource (R) (A). One hypothesis for the antagonistic interaction is that *P. aeruginosa* kills S. aureus upon contact (B). An alternative hypothesis is extracellular allelopathy, where *P. aeruginosa* secretes an extracellular compound (All) that kills *S. aureus* (C).

With the resource-limited growth and consumption assumptions made above, the rates of change in the densities of the bacterial populations and resource, in batch culture, are given by the following set of coupled ordinary differential equations:

$$\frac{dR}{dt} = \underbrace{-\psi(R)\bullet(e_{Pa}\bullet v_{Pa}\bullet N_{Pa} + e_{Sa}\bullet v_{Sa}\bullet N_{Sa})}_{Decline\ in\ Resource\ Concentration} \quad (1)$$

$$\frac{dN_{Pa}}{dt} = \underbrace{\psi(R)\bullet v_{Pa}\bullet N_{Pa}}_{Increase\ in\ P.aeruginosa\ Density} \quad (2)$$

$$\frac{dN_{Sa}}{dt} = \underbrace{\psi(R)\bullet v_{Sa}\bullet N_{Sa}}_{Increase\ in\ S.aureus\ Density} \quad (3)$$

$$where\ \ \psi(R) = \frac{R}{(R+k)} \quad (4)$$

Contact-Dependent Inhibition (CDI) (Eq. 5-8, Fig. 1B): In this model, in addition to competing through the consumption of the shared resource, the populations interact by cell-cell contact, which we assume to be a mass action process. The *S. aureus* are killed at a rate equal to the product of their densities, that of the *P. aeruginosa*, and a parameter, δ. With these definitions and assumptions, as well as those of resource concentration-dependent growth, the rates of change of the bacterial population densities and the concentration of the shared resource, in batch culture, are given by,

$$\frac{dR}{dt} = \underbrace{-\psi(R) \bullet (e_{Pa} \bullet v_{Pa} \bullet N_{Pa} + e_{Sa} \bullet v_{Sa} \bullet N_{Sa})}_{\text{Decline in Resource Concentration}} \quad (5)$$

$$\frac{dN_{Pa}}{dt} = \underbrace{\psi(R) \bullet v_{Pa} \bullet N_{Pa}}_{\text{Increase in P.aeruginosa Density}} \quad (6)$$

$$\frac{dN_{Sa}}{dt} = \underbrace{\psi(R) \bullet v_{Sa} \bullet N_{Sa} - \delta \bullet N_{Pa} \bullet N_{Sa}}_{\text{Change in S. aureus Density When Inhibited by P. aeruginosa, Upon Contact}} \quad (7)$$

$$where \ \psi(R) = \frac{R}{(R+k)} \quad (8)$$

Extracellular Allelopathy (Eq. 9-13, Fig. 1C): In addition to competing by sharing a common resource, in this model the *P. aeruginosa* population (N_{Pa}) produces an extracellular allelopathic agent (A). The *S. aureus* population is killed at a rate proportional to the concentration of A (μg/ml), its density and a rate constant, γ. The *P. aeruginosa* population produces A at a rate proportional to its rate of growth, its density, and a parameter, β. With these definitions and assumptions, as well as those of resource concentration-dependent growth, the rates of change of the bacterial population densities and the concentration of the shared resource, in batch culture, are given by,

$$\frac{dR}{dt} = \underbrace{-\psi(R) \bullet (e_{Pa} \bullet v_{Pa} \bullet N_{Pa} + e_{Sa} \bullet v_{Sa} \bullet N_{Sa})}_{\text{Decline in Resource Concentration}} \quad (9)$$

$$\frac{dN_{Pa}}{dt} = \underbrace{\psi(R) \bullet v_{Pa} \bullet N_{Pa}}_{\substack{\text{Change in P. aeruginosa} \\ \text{Density}}} \quad (10)$$

$$\frac{dN_{Sa}}{dt} = \underbrace{\psi(R) \bullet v_{Sa} \bullet N_{Sa} - \gamma \bullet N_{Sa} \bullet A}_{\substack{\text{Change in S. aureus Density When} \\ \text{Inhibited by the Allelopathic Compound}}} \quad (11)$$

$$\frac{dA}{dt} = \underbrace{\psi(R) \bullet v_{Pa} \bullet \beta \bullet N_{Pa}}_{\substack{\text{Rate of Production of} \\ \text{the Allelopathic Compound}}} \quad (12)$$

$$\text{where } \psi(R) = \frac{R}{(R+k)} \quad (13)$$

Table 1: Parameters and variables used for numerical solutions Maximum growth rates were estimated using the Bioscreen® data shown in Table 2. Initial densities of *P. aeruginosa* and *S. aureus* were estimated by plating before each experiment. "Synthetic" parameters and variables were approximated by hand in attempt to capture the dynamics observed *in vitro.* Resource concentration, conversion efficiency, and Monod constants are synthetic because the exact concentration of limiting resource in LB is unknown. The conversion efficiency of *S. aureus* is higher than that of *P. aeruginosa* because it has been observed throughout the present study that *S. aureus* grows to a lower stationary density than *P. aeruginosa*, in LB. Since densities are plotted on a log scale, an initial value of 1 is equal to an initial density of zero.

	Parameter/Variable	Description	Initial Values for Variables	Estimated Values for Parameters	Source
$\mathbf{R}$	Variable	Common Resource Concentration (μg/mL)	2500	--	Bioscreen® /Synthetic
$\mathbf{N_{Pa}}$	Variable	*P. aeruginosa* Density (CFU/mL)	Differs by Simulation	--	CFU Estimation on Agar Plates
$\mathbf{N_{Sa}}$	Variable	*S. aureus* Density (CFU/mL)	Differs by Simulation	--	CFU Estimation on Agar Plates
$\mathbf{A}$	Variable	Density of Allelopathic Agent (mL^{-1})	1	--	Synthetic
$\mathbf{v_{Pa}}$	Parameter	Maximum Growth Rate of *P. aeruginosa* (hr^{-1})	--	1.96	Bioscreen®
$\mathbf{v_{Sa}}$	Parameter	Maximum Growth Rate of *S. aureus* (hr^{-1})	--	1.96	Bioscreen®
$\mathbf{e_{Pa}}$	Parameter	Conversion Efficiency of *P. aeruginosa* (μg/cell)	--	7×10^{-7}	CFU Estimation on Agar Plates /Synthetic
$\mathbf{e_{Sa}}$	Parameter	Conversion Efficiency of *S. aureus* (μg/cell)	--	9×10^{-7}	CFU Estimation on Plates/Synthetic
$\mathbf{k}$	Parameter	Half-saturation constant for the common resource (μg/mL)	--	1000	Synthetic
$\boldsymbol{\gamma}$	Parameter	Coefficient of *S. aureus* killing by the allelopathic agent	--	1.0×10^{-8}	Synthetic
$\boldsymbol{\beta}$	Parameter	Conversion factor between the density of *P. aeruingosa* density of allelopathic agent	--	2.0×10^{-2}	Synthetic
$\boldsymbol{\delta}$	Parameter	Coefficient of *P. aeruginosa* killing *S. aureus* by cell-cell contact	--	4.0×10^{-10}	Synthetic

Estimates of Growth rates and Lag times: The estimated maximum growth rates (v_{max}) and lag times of the bacteria used in this study are presented in Table 2. One limitation with the measurements is that LB broth is a complex media, where the limiting resource is not known and may vary by species. In attempt to rectify this issue, we grew both *P. aeruginosa* and *S. aureus* in different dilutions of LB, and no growth was observed for each species, once the LB density was 1/100. This observation was taken as evidence that LB is a limiting resource and the same component of the LB complex media likely limits the growth of each species. The v_{max} for PAO1 WT is approximately the same as that of SaJE2 (two sample t-test with unequal variance: $p = 0.92$). However, the lag time of PAO1 WT is significantly longer than that of SaJE2 (two sample t-test with unequal variance: $p<0.001$). Therefore, according to the simple resource competition model, *S. aureus* should predominate in serial passage.

The parameter dynamic vary slightly with the fluorescently labelled strains. While the v_{max} for PAO1 WT is the approximately same both with and without GFP, the lag time of the GFP strain is significantly longer (two sample t-test with unequal variance: $p<0.001$). The v_{max} of PAO1 WT-GFP is significantly higher than that of SaJE2-Dsred (two sample t-test with unequal variance: $p<0.05$). The most noteworthy difference is that the PAO1 *pqsL* strain had a significantly faster v_{max} than both PAO1 WT strains (two sample t-test with unequal variance: PAO1 WT, $p<0.001$; PAO1 WT-GFP, $p<0.001$), indicating a fitness cost to the production of the *pqsL* gene product.

Table 2: Growth Parameters for Strains Used in the Study Mean ± S.E.M. shown ($N = 10$; ‡: $N=5$). Maximum growth rates (v_{max}) are defined as the instantaneous rate of change (hr^{-1}) when the cultures reached $OD_{600} = 0.02$. Lag times were defined as the amount of time (hr) until the cultures reached $OD_{600} = 0.02$.

Strain	v_{max} (hr^{-1})	Lag (hr)
PAO1 WT	1.96 ± 0.03	3.62 ± 0.01
Sa JE2	1.96 ± 0.03	2.67± 0.02
PAO1 WT (GFP)	2.03 ± 0.06	4.35± 0.01
PAO1 pqsL (GFP)‡	2.95 ± 0.26	4.58 ± 0.20
Sa JE2 (Dsred)	1.88 ± 0.07	3.67± 0.00

Numerical Solutions – Simulations: The above equations, and those that follow, were solved numerical Berkeley Madonna software version 9.1.14. To simulate the serial transfer mode of population maintenance, every 24 hours, the densities of the simulated populations were reduced by a factor of 1000, and fresh resources were supplied. Lags were simulated by initiating the growth of the population after the given amount of time following the start of each transfer. The growth rate lag times used for the following simulations are depicted in Table 2.

Simulations of Simple Resource Competition: In Figure 2, we present the results of simulations of the model depicted in Figure 1A, where the populations interact solely by consumption of the common resource. Since *P. aeruginosa* and *S. aureus* were measured to have the same v_{max} and *S. aureus* has a shorter lag time than *P. aeruginosa*, *S. aureus* is hypothesized to grow to higher frequency than *P. aeruginosa*.

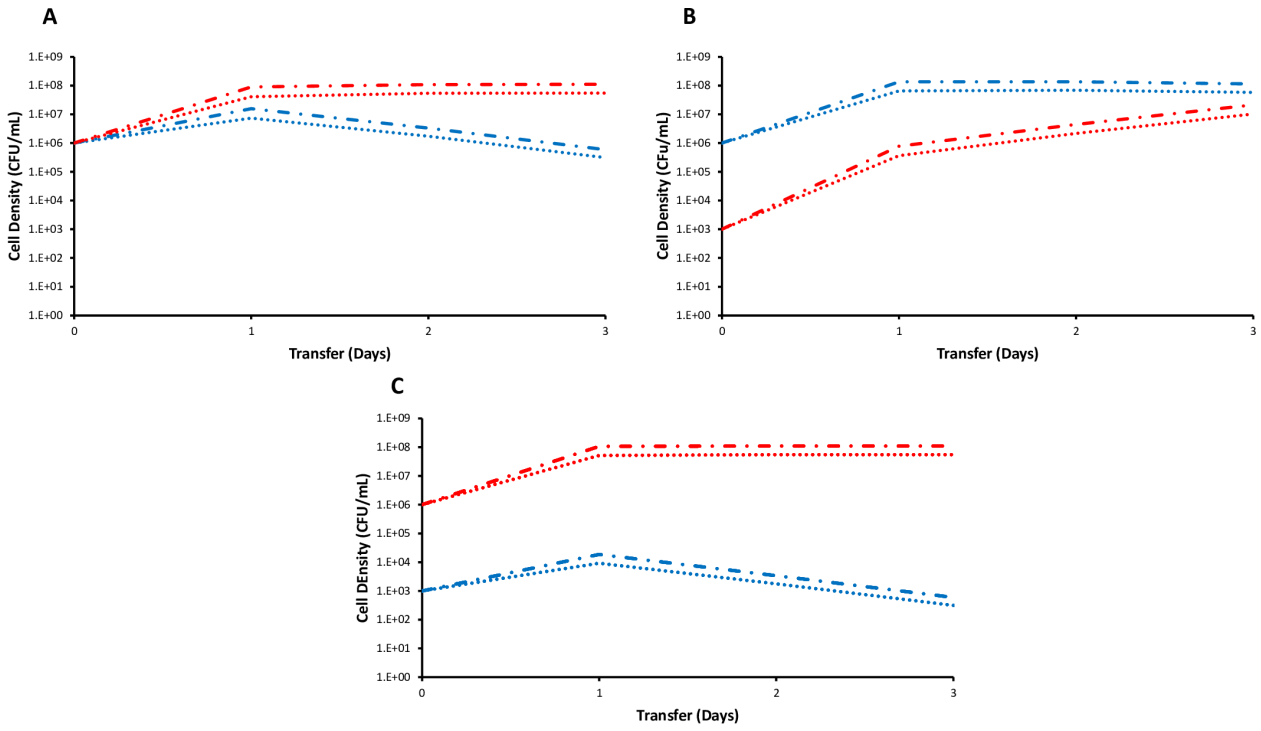

Figure 2: Simulations of resource competition (Fig. 1A) Changes in the densities of the bacterial populations in serial transfer culture using common *P. aeruginosa* (blue) and *S. aureus* (red) at different initial frequencies: *P. aeruginosa* initially equal (A), high (B), and rare (C). Dashed lines

represent a simulation with a resource concentration of 100 μg/mL and the dotted lines represent a resource concentration of 50 μg/mL. The v_{max} and lag time values used are those in Table 2. The *S. aureus* population increases in frequency for each initial condition.

Serial Passage: Demonstrating the Frequency and Density Dependence of Antagonism in Liquid Culture: To evaluate the validity of the simple resource competition model in Fig. 1A, we performed an *in vitro* serial passage competition experiment between *P. aeruginosa* and *S. aureus*.

Pure, stock cultures of PAO1 WT and SaJE2 were prepared and sampled the next day, to measure initial cell densities. For the 1:1 (PAO1 WT : SaJE2 ratio) 100 µL of 1/100 stationary culture dilution, for each species, was transferred into 3 mL of LB broth. In the 1:0.001 and 0.001:1 mixtures 100 µL of 1/100 stationary culture dilution of the more concentrated species was transferred, while 100 µL of 1/10,000 stationary culture dilution of the less concentrated species was added to 3 mL of LB broth. Single-clone controls for each species were also initiated in the same manner. Experiments were carried out in plastic 12-well plates and incubated over night at 37˚ C, with shaking. The following day, the LB broth cultures were sampled on plates.

In single-clone cultures started at approximately equal initial densities ($D_{0\text{-strain}}$ CFU/mL), *P. aeruginosa* PAO1 WT and *S. aureus* JE2 both grow to the same stationary density ($D_{n\text{-strain}}$, where n = passage number in days) after three serial passages ($D_{3\text{-PAO1(N=2)}}$ = 2E9 ± 8E8 CFU/mL, $D_{3\text{-SaJE2 (N=3)}}$ = 2E9 ± 4E7 CFU/mL, two-sample t-test, assuming unequal variance, p =1.00) (Fig. 3A and 3B).

However, when placed in a mixed culture at approximately equal initial density, the population of *S. aureus* does not significantly increase relative to the initial density in the first passage ($D_{0\text{-SaJE2(N=3)}}$= 3E6 ± 3E6 CFU/mL, $D_{1\text{-SaJE2(N=3)}}$= 3E7 ± 2E7 CFU/mL, paired two-sample t-test, p = 0.31). By the second passage, *S. aureus* is completely eradicated, while the density of *P. aeruginosa* remains similar to that of the single-clone cultures (PAO1 Single vs. Mix: $D_{2\text{-PAO1-SINGLE(N=3)}}$ = 2E9 ± 9E7 CFU/mL, $D_{2\text{-PAO1-MIX}}$ = 3E9 ± 7E8 CFU/mL, two-sample t-test with unequal variance, p = 0.23; PAO1 Mix vs. SaJE2 Mix: $D_{2\text{-PAO1-MIX(N=3)}}$ = 3E9 ± 7E8 CFU/mL,

$D_{2\text{-SaJE2-MIX(N=3)}}$ = 0 ± 0 CFU/mL, two-sample t-test, assuming unequal variance, p =0.01). (Fig. 3C).

When *S. aureus* is initially rare in the population ($D_{0\text{-PAO1}}$: $D_{0\text{-SaJE2}}$ ~ 1 : 0.001), similar dynamics are observed (Fig. 3D). The *S. aureus* density does not significantly increase after the first passage ($D_{0\text{-SaJE2(N=3)}}$ = 4E3 ± 2E3 CFU/mL, $D_{1\text{-SaJE2(N=3)}}$ = 1E4 ± 1E4 CFU/mL, paired two-sample t-test, p = 0.41) and is completely eradicated after the second passage. *P. aeruginosa* does not exhibit different dynamics than if it were alone at the second passage, while *S. aureus* is eradicated (PAO1 Single vs. PAO1 Mix: $D_{2\text{-PAO1-SINGLE(N=3)}}$ = 2E9 ± 9E7 CFU/mL, $D_{2\text{-PAO1-MIX}}$ = 3E9 ± 6E8 CFU/mL, two-sample t-test, assuming unequal variance, p = 0.17; PAO1 Mix vs. SaJE2 Mix: $D_{2\text{-PAO1-MIX(N=3)}}$ = 2E9 ± 9E7 CFU/mL, $D_{2\text{-SaJE2-MIX(N=3)}}$ = 0 ± 0 CFU/mL, two-sample t-test, assuming unequal variance, p <0.001).

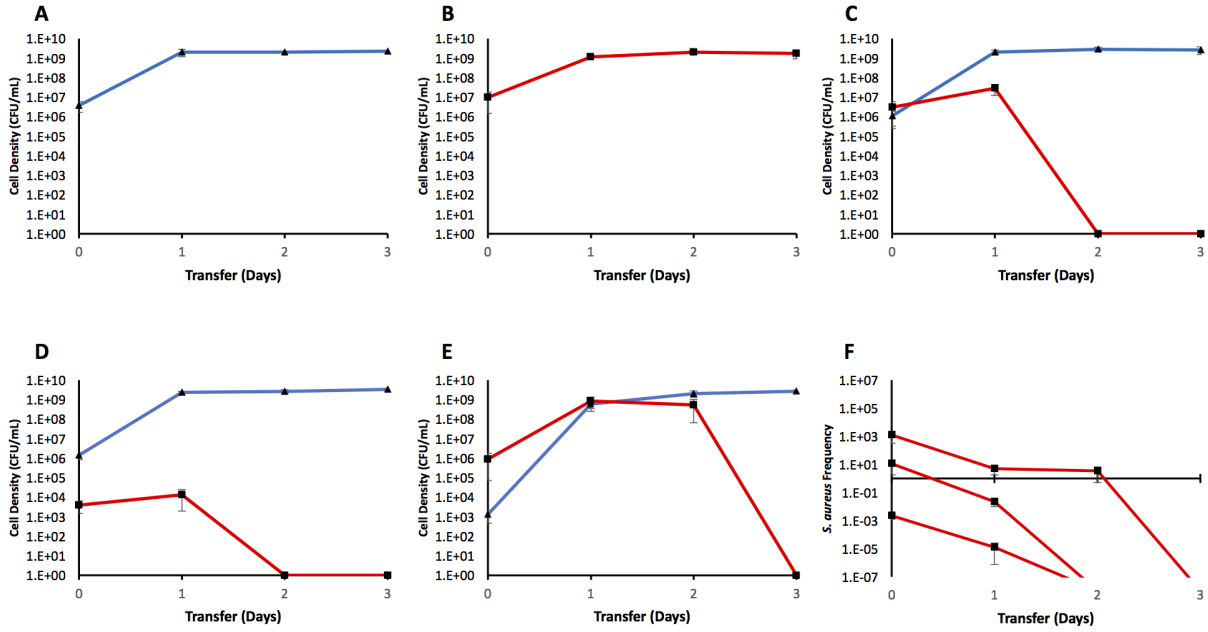

Figure 3: *S. aureus* JE2 decline and eradication during serial passage with *P. aeruginosa* PAO1 occurs in a frequency-dependent manner The means of three independent experiments are shown in each graph. Error bars represent the S.E.M. PAO1 (blue triangles) and SaJE2 (red squares) grow to the same stationary density when serial passaged as single-clone cultures (A and B). In each mixed culture, PAO1 is the predominant species population by the third passage. When PAO1 and *S. aureus* JE2 (blue squares) are mixed in a ~1 : 1 ratio (C) and a ~1 : 0.001 (PAO1 : JE2) ratio (D), *S. aureus* is eradicated by the second passage. However, when PAO1 is initially

rare (~0.001 : 1, PAO1 : JE2), the PAO1 reaches approximately the same density as the *S. aureus* after the first and second passages, and eventually overtakes the culture at the third passage (E). F shows the ratio of *S. aureus* to *P. aeruginosa* for each of the initial frequencies, throughout all three passages.

When *P. aeruginosa* is initially rare ($D_{0\text{-PAO1}}$: $D_{0\text{-SaJE2}} \sim 0.001 : 1$), different, though consistent, dynamics occur (Fig. 3E). Both the *P. aeruginosa* and *S. aureus* increase after the first passage, but this difference is not statistically significant for *P. aeruginosa* ($D_{0\text{-PAO1}(N=3)}$ = 1E3 ± 9E2 CFU/mL, $D_{1\text{-PAO1}(N=3)}$ = 5E8 ± 2E8 CFU/mL, paired two-sample t-test, p =0.20; $D_{0\text{-SaJE2}(N=3)}$= 9E5 ± 8E5 CFU/mL, $D_{1\text{-SaJE2}(N=3)}$ = 9E8 ± 5E8 CFU/mL, paired two-sample t-test, p =0.23). Between passages 1 and 2, the populations of each species are the same relative to members of the same species and across species (PAO1: $D_{1\text{-PAO1}(N=3)}$= 6E8 ± 3E8 CFU/mL, $D_{2\text{-PAO1}(N=3)}$= 2E9 ± 7E8 CFU/mL, paired two-sample t-test, p =0.11; SaJE2: $D_{1\text{-SaJE2}(N=3)}$ = 9E8 ± 5E8 CFU/mL, $D_{2\text{-SaJE2}}$ = 5E8 ± 5E8 CFU/mL, paired two-sample t-test, p =0.40; Passage 1 PAO1 vs. $\text{SaJE2}_{(N=3)}$: two-sample t-test, assuming unequal variance, p =0.52; Passage 2 PAO1 vs. $\text{SaJE2}_{(N=3)}$: two-sample t-test, assuming unequal variance, p =0.25). At passage 3, the *S. aureus* are completely eradicated and the *P. aeruginosa* density remains similar to the passage 3 single-clone density (PAO1 Single vs. PAO1 Mix: $D_{3\text{-PAO1-SINGLE}(N=2)}$ = 2E9 ± 4E7 CFU/mL, $D_{3\text{-PAO1-Mix}(N=3)}$ = 3E9 ± 4E8 CFU/mL, two-sample t-test, assuming unequal variance, p =0.13; PAO1 Mix vs. SaJE2 Mix: $D_{3\text{-PAO1-MIX}(N=2)}$ = 3E9 ± 4E8 CFU/mL, $D_{3\text{-SaJE2-MIX}(N=2)}$ = 0 ± 0 CFU/mL, two-sample t-test, assuming unequal variance, p =0.02). By making *P. aeruginosa* rare, the eradication of *S. aureus* is delayed by one passage.

<u>Modelling the Observed Antagonism Using an Extracellular Allelopathy or CDI Framework:</u>
Based on the results of the liquid serial passage experiment, it is evident that simple resource competition (Fig. 1A) cannot explain the observed dynamics. To explain *P. aeruginosa* antagonism towards *S. aureus*, we simulate the models shown in Fig. 1B and 1C.
When comparing the results of these models, there are three issues that arise (Fig. 4). The first problem is that simulated results generated from these models cannot be distinguished based on population data. There exist parameters for each that would yield nearly identical population dynamics (Fig. 4). Second, the models are not mutually exclusive: There may be some

components that are extracellular and others that are contact-dependent. To determine whether the mechanism is solely extracellular, requires contact between cells, or both, experiments comparing *S. aureus* growth in cell-free *P. aeruginosa* extracts to growth in the presence of living *P. aeruginosa* cells are necessary. Third, *P. aeruginosa* cannot predominate in serial passage, if initially rare, which is in direct conflict with the experimental observations. Explanation of the rare *P. aeruginosa* advantage observation requires an expansion of the base models.

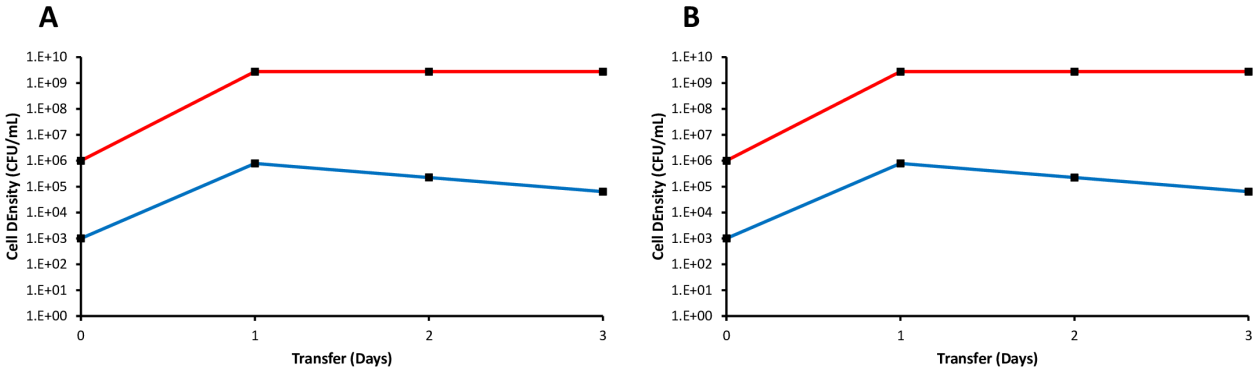

Figure 4: <u>In extracellular allelopathy and contact-dependent models, *P. aeruginosa* cannot predominate if initially rare, and the two models can exhibit indistinguishable dynamics</u>
Simulated data from the extracellular allelopathy (A, Fig. 1C) and contact-dependent (B, Fig. 1B) models. (*P. aeruginosa*=blue, *S. aureus*=red.)

<u>Short-Term Growth Experiment: Determining the Time of Inhibition:</u> Another possible way of distinguishing between extracellular allelopathy and CDI is the time in the growth cycle in which the inhibition occurs. Late growth cycle inhibition is consistent with other known CDI mechanisms [19, 20]. Declines in *S. aureus* density due to *P. aeruginosa* have been previously shown to occur late in growth [12]. In the next experiment, we aim to replicate this result in LB media.

Pure cultures were prepared of *P. aeruginosa* PAO1 WT and *S. aureus* JE2. The overnight cultures were serially diluted and sampled. 100 µL of 1/100 dilution for each species was added

to 10 mL of LB broth to create the following cultures, in covered 25 mL Erylenmeyer flasks: PAO1 alone, *S. aureus* JE2 alone, PAO1/*S. aureus* JE2 (~1:1) mixture.

To characterize the competition early in the growth cycle, the cultures were placed in a 37˚ C gyrating water bath. 100 µL of each culture was serially diluted and sampled every 30 minutes onto LB agar MSA plates, for 5 hours. These plates were placed in the incubator overnight, at 37˚ C. The cultures were left in the water bath for one night and sampled the next day on LB agar and MSA plates. The plates were placed in the incubator over night, at 37˚ C, and cell densities were estimated the next day. The cultures were left in the water bath for another 24 hours and sampled again on LB agar and MSA plates.

To examine the competition late in the growth cycle, the identical experimental conditions were prepared late in the day and placed in the incubator for the night, with shaking. The next morning, 10 hours after the sample was prepared, 100 µL of each culture was serially diluted and sampled on LB agar and MSA plates. Cell densities were estimated the next day. This protocol was repeated every hour for 5 hours.

When started at approximately equal initial densities, *P. aeruginosa* and *S. aureus* grow similarly at the beginning of the growth cycle. However, late in the growth cycle, *S. aureus* population declines, reaching a final density of 8E5 CFU/mL at t=15 hr. (Fig. 5). The *S. aureus* density was approximately the same values at t = 48 hr.

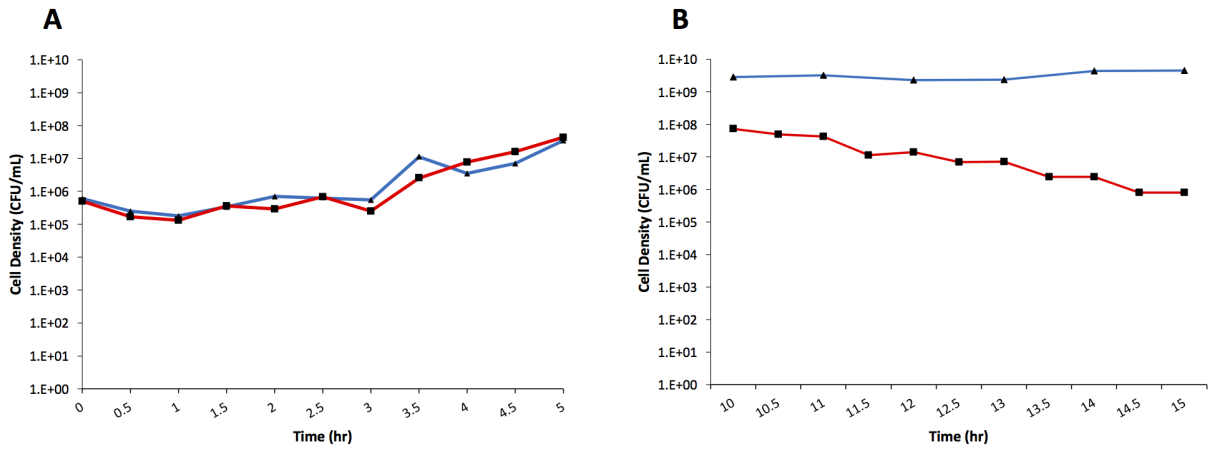

Figure 5: *P. aeruginosa* antagonism towards *S. aureus* occurs late in the growth cycle Data from one experiment are shown. Cultures were sampled every 30 min. Early in the early growth

cycle, *P. aeruginosa* (blue triangles) and *S. aureus* (red squares) grow similarly (A). However, the *S. aureus* density declines approximately 100-fold late in the growth cycle and remains at approximately the same reduced value 48 hr after the cultures were initiated (B).

Table 3: <u>Enriched Media Experiments</u>: Pure stock cultures of PAO1 WT, PAO1 *pqsL*, and SaJE2 were prepared in 25 mL of LB inside covered 300 mL Erlenmeyer flasks. The following day, 10 mL of the overnight PAO1 WT and PAO1 *pqsL* cultures were sonicated with a Branson Sonifier® 250A for 1 minute, by alternating between 10 seconds of sonication and 10 seconds of rest for six cycles. The sonicated cultures were then centrifuged for 10 minutes at 14,000 rpm. The supernatants were passed through 0.2 µm filters, approximately 1.5 mL at a time, and centrifuged once more for 10 minutes at 14,000 rpm. The re-spun supernatants were passed through fresh 0.2 µm filters. A new filter and syringe were used approximately every 1.5 mL. 100 µL of 1/100 dilutions of *P. aeruginosa* and/or *S. aureus* overnight cultures were transferred to make the experimental conditions summarized in Table 3. Non-replicating cultures consisted of the undiluted, overnight *P. aeruginosa* cultures used to prepare the supernatants. 1.75 mL of supernatant and stationary culture was used; 1 mL of 2x concentrated LB was used; 2 mL of MSB was used. The following day, the cultures were sampled. (SUP = supernatant; LB = Lysogeny Broth; MSB = Mannitol Salt Broth; 2xLB = 2x concentrated LB, STAT=non-replicating culture.)

PAO1 WT + 2xLB
PAO1 *pqsL* + 2xLB
SaJE2 + 2xLB
PAO1 WT + SaJE2 + 2xLB
PAO1 *pqsL* + SaJE2 + 2xLB
PAO1 WT + PAO1 WT-SUP + 2xLB
PAO1 *pqsL* + PAO1 *pqsL*-SUP + 2xLB
SaJE2 + PAO1 WT-SUP + 2xLB
SaJE2 + PAO1 *pqsL*-SUP + 2xLB
SaJE2 + MSB
Sa JE2 + PAO1 WT-STAT + MSB
Sa JE2 + PAO1 *pqsL*-STAT + MSB
Sa JE2 + PAO1 WT-SUP + MSB
Sa JE2 + PAO1 *pqsL*-SUP + MSB

S. aureus Growth in Enriched 2xLB (Fig. 6A, Table 3): Based on the short-term competition experiment, and the results of previous studies, *P. aeruginosa* antagonism towards *S. aureus* occurs late in the growth cycle. This observation is consistent with what has been observed in other CDI systems. However, the present study must definitively demonstrate whether contact between individuals of each species is necessary to observe the full extent of the antagonistic interaction.

By growing *S. aureus* in sonicated cell-free extracts of *P. aeruginosa* PAO1 WT and PAO1 *pqsL*, we can determine whether the interaction has a molecular component. However, based on these experiments alone, we cannot address whether contact-based inhibition also occurs, or if the molecules present in the supernatants are normally delivered via a contact-dependent secretion system. Both sonicated PAO1 WT and PAO1 *pqsL* supernatants do not affect the ratio of recovered to initial density (D_f/D_i) of SaJE2, relative to the control condition of single-clone SaJE2. However, when approximately equal initial densities of PAO1 and SaJE2 are mixed in 2xLB, the D_f/D_i ratio for SaJE2 is significantly lower in both the WT and *pqsL* co-cultures than in the single-clone control (SaJE2-Alone$_{(N=5)}$: 1E3 ± 1E2; vs. SaJE2+PAO1 WT$_{(N=2)}$: 1E2 ± 6E1, two sample, unpaired t-test, assuming unequal variance, $p<0.001$; vs. SaJE2 + PAO1 *pqsL*$_{(N=2)}$: 3E2 ± 2E2, two sample, unpaired t-test, assuming unequal variance, $p<0.05$). In addition, the D_f/D_i ratios for SaJE2 in co-culture with PAO1 WT and that when grown in the presence of PAO1 WT sonicated supernatant are significantly different (vs. SaJE2 + PAO1 WT-SUP$_{(N=5)}$, 1E3 ± 4E2, two sample, unpaired t-test, assuming unequal variance: $p<0.05$). There is no significant difference between in the D_f/D_i ratios for SaJE2 alone and when grown in the presence of either PAO1 supernatant. Since the full extent of the antagonism is dependent upon the presence of living cells, there must be an interspecies interaction, and an extracellular allelopathy model where the release of the toxic agent is only dependent upon the density of *P. aeruginosa* is insufficient.

S. aureus Growth in the Presence of Non-Replicating *P. aeruginosa* (Enriched MSB Media) (Fig. 6B, Table 3): To determine if interspecies, intercellular interactions play a role in the inhibition, we grow *S. aureus* in the presence of non-replicating *P. aeruginosa*. We ensure that *P. aeruginosa* does not grow in these experiments by using MSB as the culture medium, where only *S. aureus* can grow. An important feature of this non-replicating *P. aeruginosa* is that it comes from the same, undiluted cultures that were used to prepare the supernatants. Therefore, the only presumable differences between the contents of the non-replicating *P. aeruginosa* and the sonicated *P. aeruginosa* supernatants are the presence of the living cells and the existence of any intracellular compounds liberated by sonication. Differences between *S. aureus* growth with and without viable *P. aeruginosa* cells can be characterized as evidence for intercellular interaction between species, either taking the form of contact-dependent inhibition or cross-species induction of genes responsible for the antagonism.

Neither strain of PAO1 grows in MSB, while SaJE2 grows in MSB, but to a significantly lower density than it does in 2xLB (SaJE2 + $MSB_{(N=3)}$: 3E7 ± 2E7 CFU/mL; SaJE2 + $2xLB_{(N=5)}$: 2E9 ± 5E8 CFU/mL; two sample, unpaired t-test, assuming unequal variance: $p<0.05$). When cultured in the presence of stationary phase PAO1 WT, the recovered density of SaJE2 is lower than the initial density (i.e. $D_f/D_i < 1$) (SaJE2 + PAO1 WT-$STAT_{(N=3)}$: 2E-2 ± 5E-3), implying that the *S. aureus* cells were killed in the presence of PAO1 WT. This ratio is lower than both that of SaJE2 grown in MSB alone and SaJE2 cultured in the presence of PAO1 WT sonicated supernatant (SaJE2 + $MSB_{(N=3)}$: 2E1± 1E1; SaJE2 + PAO1 WT-$SUP_{(N=3)}$: 2E2± 1E2). There is no evidence of *S. aureus* killing when mixed with non-replicating PAO1 *pqsL* or PAO1 *pqsL* supernatant. However, the growth of *S. aureus* is less than the single-clone control when cultured in the presence of non-replicating PAO1 *pqsL.*

These results are consistent with those in 2xLB, as it is evident that living cells are necessary for *S. aureus* killing by *P. aeruginosa*. It is also evident that HQNO plays a role in the antagonistic interaction, as the *pqsL* mutant displayed reduced inhibition, even with living cells present.

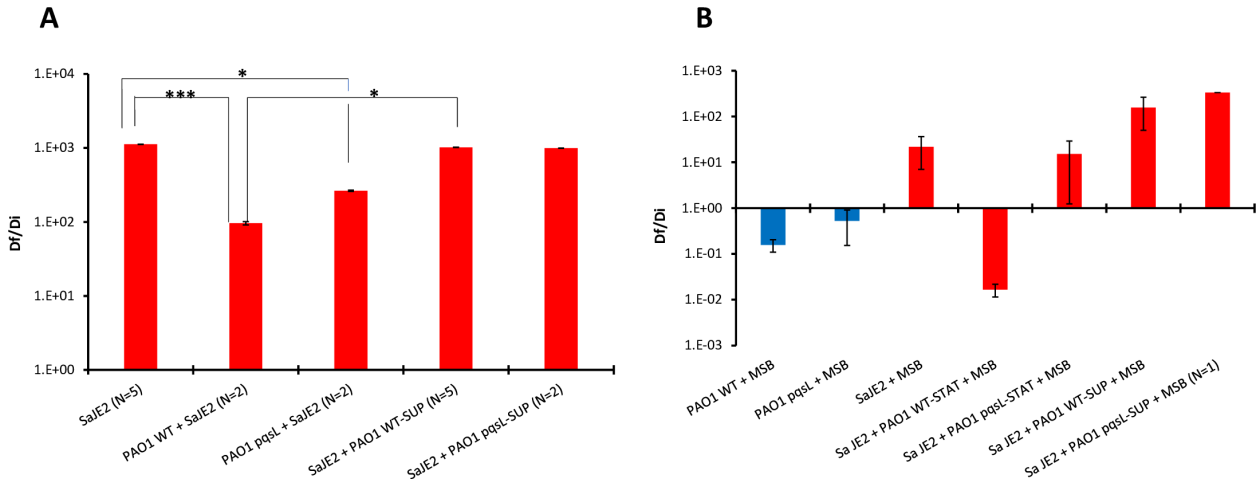

Figure 6: *P. aeruginosa* antagonism involves direct killing of *S. aureus* and requires the presence of both living *P. aeruginosa* cells and HQNO The mean ratio of the final density to the initial cell density (D_f/D_i), for three independent experiments, is shown, unless otherwise specified. (SUP=sonicated supernatant, STAT=stationary phase culture.) Red bars represent D_f/D_i ratios for *S. aureus* and blue bars represent the *P. aeruginosa* ratios. Error bars represent the S.E.M. Statistically significant differences are marked (*, $p<0.05$; **, $p<0.01$; ***, $p<0.001$). When grown in 2xLB, the *S. aureus* D_f/D_i ratio is significantly lower when supplemented with living PAO1 WT, or living PAO1 *pqsL,* than it is when alone or cultured in the presence of PAO1 WT sonicated supernatant (A). In addition, there are no significant differences in the S. *aureus* D_f/D_i ratios between either sonicated PAO1 supernatant condition and the single-species control, in 2xLB (A). When grown in MSB, *P. aeruginosa* density either remains constant or reduced relative to the initial density, while *S. aureus* grows (B). *S. aureus* grows in MSB in the presence of PAO1 WT sonicated supernatant, PAO1 *pqsL* sonicated supernatant, and non-replicating PAO1 *pqsL* living cells (B). When grown in MSB, in the presence of non-replicating PAO1 WT, the *S. aureus* density declines ~200-fold (B).

Short-Term Growth Experiment in the Presence of Enriched 2xLB (Fig. 7): Based on the previous two experiments, it is evident that the presence of sonicated *P. aeruginosa* supernatant does not significantly affect the recovered cell densities of *S. aureus*. However, these data do not address whether the supernatants give *S. aureus* a growth disadvantage by lowering the v_{max} or increasing the lag time. Short-term growth experiments examining the change in OD_{600} of *S. aureus* in the presence of sonicated *P. aeruginosa* supernatant are necessary to determine the

existence of this phenomenon. When grown in the presence of PAO1 WT 1:1 (SUP:2xLB), SaJE2 has a slower v_{max} and longer lag time than when grown alone in liquid LB (v_{max}: SaJE2 +LB, Table 2; SaJE2 + PAO1-WT (SUP), 1.37 ± 0.13, two-sample t-test with unequal variance, $p<0.001$; lag time: SaJE2 +LB, Table 2; SaJE2 + PAO1-WT (SUP), 6.58 ± 0.16, two-sample t-test with unequal variance, $p<0.001$) (Fig. 1). However, if grown in the presence of PAO1 *pqsL* 1:1 (SUP:2xLB), neither the v_{max} nor the lag time change significantly in comparison to the SaJE2 single-clone control (Fig. 7).

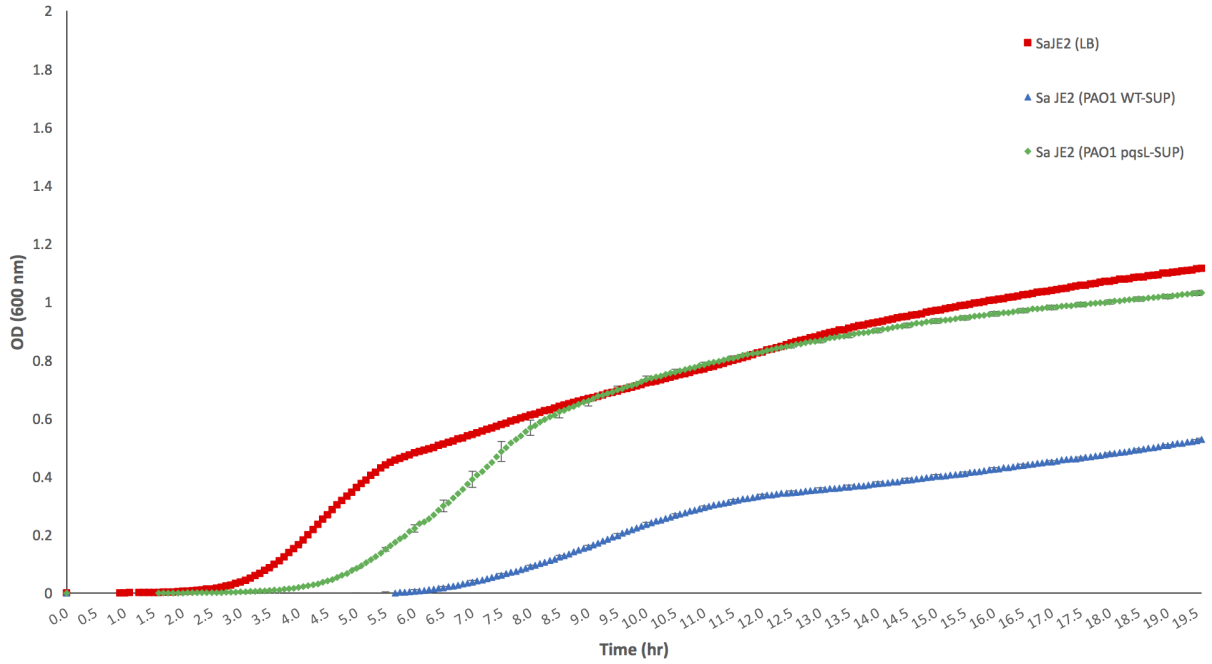

Figure 7: *S. aureus* JE2 has a growth disadvantage in the presence of sonicated PAO1 WT supernatant OD_{600} values were taken every 5 minutes for approximately 20 hours. The mean of 10 replicates is shown. Error bars are shown at each half hour and represent the S.E.M. *S. aureus* was grown alone in LB (red squares), with a 1:1 ratio of 2xLB and PAO1 WT supernatant (blue triangles), and with a 1:1 ratio of 2xLB and PAO1 *pqsL* supernatant (green diamonds). The v_{max} of *S. aureus* is lowered and the lag time is increased when cultured with PAO1 WT sonicated supernatant. The *S. aureus* lag time slightly longer in the presence of PAO1 *pqsL* supernatant, but the v_{max} is unaltered.

From these past three experiments, it appears that the antagonism of *P. aeruginosa* towards *S. aureus* is dependent upon an interaction between the two species and the presence of HQNO. This result is complicated based on the short-term growth experiment, as there appears to exist a layer of the mechanism that is HQNO-dependent, independent of the presence of *S. aureus,* and that is acting towards *S. aureus* in a growth static manner. It could also be that the mechanism that leads to this short-term growth disadvantage is the same as that that leads to the killing of *S. aureus*, but that the presence of viable *S. aureus* cells amplifies this mechanism.

Interspecies dependence can be modelled as direct killing upon contact, as is shown in Fig. 1B, or production of an extracellular agent that is dependent upon a cross-species interaction between cells. In the former scenario, it is also possible that there is a contact-dependent killing mechanism that involves *P. aeruginosa* directly injecting toxic exoproduct(s), such as HQNO, into *S. aureus* via a secretion system.

Using Interspecies Interactions to Model the Rare *P. aeruginosa* Advantage: The observation of interspecies dependence alone fails to address the biggest problem with the antagonism models diagrammed in Fig. 1B and 1C. That is, if initially rare, *P. aeruginosa* cannot overtake the population (Fig. 4). This property is contrary to what is observed experimentally in Fig. 3E. Mashburn et al., 2005 presented evidence that *P. aeruginosa* lyses *S. aureus* to obtain iron as an additional resource, much like a predator-prey relationship. This phenomenon can be added to the contact-dependent (Eq. 14-18, Fig. 8A) and extracellular allelopathy (Eq. 19-24, Fig. 8B) models by creating a new resource that is yielded from *P. aeruginosa* killing *S. aureus* (R_{Sa}). The rate of appearance of this resource is proportional to the death of *S. aureus*, and this new resource can only be utilized by *P. aeruginosa*. With this addition to the models, *P. aeruginosa*, when initially rare, can increase in frequency, and eventually overtake the population. Furthermore, parameters can be estimated that approximate the dynamics observed in the serial passages with initial frequencies of 1:1 and 1:0.001 (*P. aeruginosa*:*S. aureus*). Simulations from the contact-dependent predation model are shown in Fig. 9. New parameters and variables for these models are shown in Table 4.

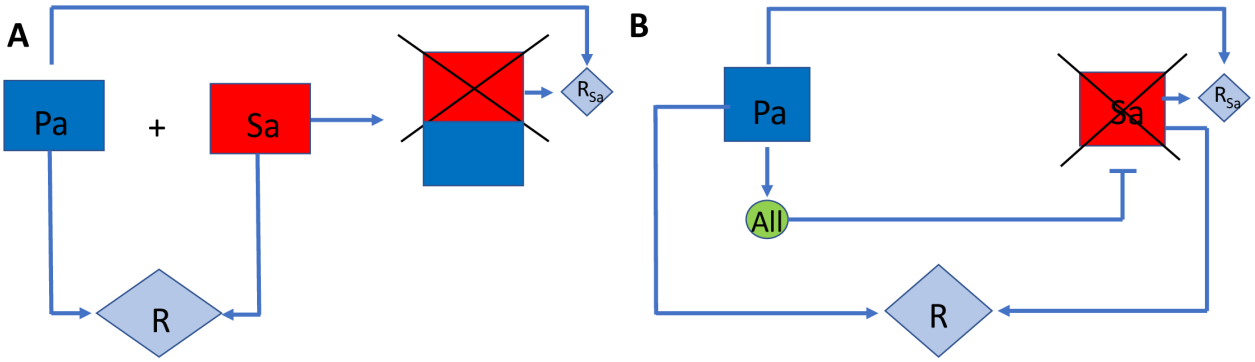

Figure 8: <u>Schematic diagrams of "predation" models</u> Contact-dependent (A) and extracellular allelopathy (B) models are adapted such that *S. aureus* (Sa) becomes a resource (R_{Sa}) for *P. aeruginosa* (Pa), upon death..

<u>Predation-Based CDI Model (Eq. 14-18, Fig. 8A)</u>: Like the earlier models, *P. aeruginosa* and S. *aureus* interact through utilization of the shared resource (R). This model is an expanded version of the one shown in Fig. 1B, and described in Eq. 5-8, where *P. aeruginosa* kills *S. aureus* upon contact. This is modelled assuming mass action, where the rate of killing is proportional to the product of the *P. aeruginosa* (N_{Pa}) and *S. aureus* (N_{Sa}) densities. This new model differs from that shown in Fig. 1B because when the populations of *P. aeruginosa* and *S. aureus* come into contact, *S. aureus* is converted into a resource (R_{Sa}). The density of R_{Sa} is defined by the product of N_{Pa}, N_{Sa}, and the two parameters, l and δ. In addition to utilizing the common resource, *P. aeruginosa* can use R_{Sa} as a resource for growth at a rate proportional to a Monod function separate to that of the common resource ($\Psi(R_{Sa})$). With these definitions and assumptions, as well as those of resource concentration-dependent growth, the rates of change of the bacterial population densities and the concentration of the shared resource, in batch culture, are given by,

$$\frac{dR}{dt} = \underbrace{-\psi(R)\bullet(e_{Pa}\bullet v_{Pa}\bullet N_{Pa} + e_{Sa}\bullet v_{Sa}\bullet N_{Sa})}_{\text{Decline in Resource Concentration}} \quad (14)$$

$$\frac{dR_{Sa}}{dt} = \underbrace{l\bullet\delta\bullet N_{Pa}\bullet N_{Sa} - \psi\left(R_{Sa}\right)\bullet e_{Pa}\bullet v_{Pa}\bullet N_{Pa}}_{\substack{\text{Change in Concentration of the Resource} \\ \text{Derived From Lysis of } S.\,aureus \text{ Cells}}} \quad (15)$$

$$\frac{dN_{Pa}}{dt} = \underbrace{\left(\psi(R) + \psi(R_{Sa})\right)\bullet v_{Pa}\bullet N_{Pa}}_{\substack{\text{Increase in } P.\,aeruginosa \\ \text{Density}}} \quad (16)$$

$$\frac{dN_{Sa}}{dt} = \underbrace{\psi(R)\bullet v_{Sa}\bullet N_{Sa} - \delta\bullet N_{Pa}\bullet N_{Sa}}_{\substack{\text{Change in } S.\,aureus \text{ Density When} \\ \text{Inhibited by } P.\,aeruginosa, \text{ Upon Contact}}} \quad (17)$$

$$\text{where } \psi(R) = \frac{R}{(R+k)} \quad \text{and} \quad \psi(R_{Sa}) = \frac{R_{Sa}}{(R_{Sa}+k_{Sa})} \quad (18)$$

Predation-Based Extracellular Allelopathy Model (Eq. 19-24, Fig. 8B): *P. aeruginosa* and *S. aureus* compete for the shared resource (R). This model is an expanded version of the one shown in Fig. 1C, and described in Eq. 9-13, where *P. aeruginosa* produces an extracellular compound at a rate defined by the product of the of *P. aeruginosa* population density (N_{Pa}) and the parameter, β. This is modelled assuming mass action, where the rate of killing is proportional to the product of the densities of (N_{Pa}), *S. aureus* (N_{Sa}) and allelopathic agent (A). This model differs from that in Fig. 1C because when the allelopathic agent kills *S. aureus*, *S. aureus* is converted into a resource (R_{Sa}). The density of R_{Sa} is defined as the product of A, N_{Sa}, and the two parameters, l and γ. In addition to utilizing the common resource, *P. aeruginosa* can use R_{Sa} as a resource for growth at a rate proportional to a Monod function separate to that of the common resource ($\Psi(R_{Sa})$). With these definitions and assumptions, as well as those of resource concentration-dependent growth, the rates of change of the bacterial population densities and the concentration of the shared resource, in batch culture, are given by,

$$\frac{dR}{dt} = \underbrace{-\psi(R)\bullet(e_{Pa}\bullet v_{Pa}\bullet N_{Pa} + e_{Sa}\bullet v_{Sa}\bullet N_{Sa})}_{\text{Decline in Resource Concentration}} \quad (19)$$

$$\frac{dR_{Sa}}{dt} = \underbrace{l\bullet\gamma\bullet A\bullet N_{Sa} - \psi\left(R_{Sa}\right)\bullet e_{Pa}\bullet v_{Pa}\bullet N_{Pa}}_{\text{Change in Concentration of the Resource Derived From Lysis of } S.\text{ aureus Cells}} \quad (20)$$

$$\frac{dN_{Pa}}{dt} = \underbrace{\left(\psi(R)+\psi(R_{Sa})\right)\bullet v_{Pa}\bullet N_{Pa}}_{\text{Change in } P.\text{aeruginosa Density}} \quad (21)$$

$$\frac{dN_{Sa}}{dt} = \underbrace{\psi(R)\bullet v_{Sa}\bullet N_{Sa} - \gamma\bullet N_{Sa}\bullet A}_{\text{Change in } S.\text{ aureus Density When Inhibited by the Allelopathic Compound}} \quad (22)$$

$$\frac{dA}{dt} = \underbrace{\left(\psi(R)+\psi(R_{Sa})\right)\bullet v_{Pa}\bullet\beta\bullet N_{Pa}}_{\text{Rate of Production of the Allelopathic Compound}} \quad (23)$$

$$where\ \ \psi(R) = \frac{R}{(R+k)} \quad and \quad \psi(R_{Sa}) = \frac{R_{Sa}}{(R_{Sa}+k_{Sa})} \quad (24)$$

Table 4: Parameters and Variables for Predation and Passively Released *S. aureus* Resource Models

	Parameter/Variable	Description	Initial Values for Variables	Estimated Values for Parameters	Source
$\mathbf{R_{Sa}}$	Variable	Concentration of Resource Derived From *S. aureus* (μg/mL)	1	--	Synthetic
$\mathbf{k_{Sa}}$	Parameter	Half-saturation constant for resource derived from *S. aureus* (μg/mL)	--	100	Synthetic
l	Parameter	Conversion factor between the density of *S. aureus* and amount of resource derived from *S. aureus*	--	1×10^{-6} (Predation Models) 1×10^{-8} (Passive Resource Models)	Synthetic
$\boldsymbol{\gamma}$	Parameter	Coefficient of *S. aureus* killing by the allelopathic agent	--	2.5×10^{-7} (Predation Model) 8.0×10^{-7} (Passive Resource Model)	Synthetic
$\boldsymbol{\beta}$	Parameter	Conversion factor between the density of *P. aeruingosa* density of allelopathic agent	--	1×10^{-3}	Synthetic
$\boldsymbol{\delta}$	Parameter	Coefficient of *P. aeruginosa* killing *S. aureus* by cell-cell contact	--	$1.5\text{-}4.5 \times 10^{-10}$	Synthetic

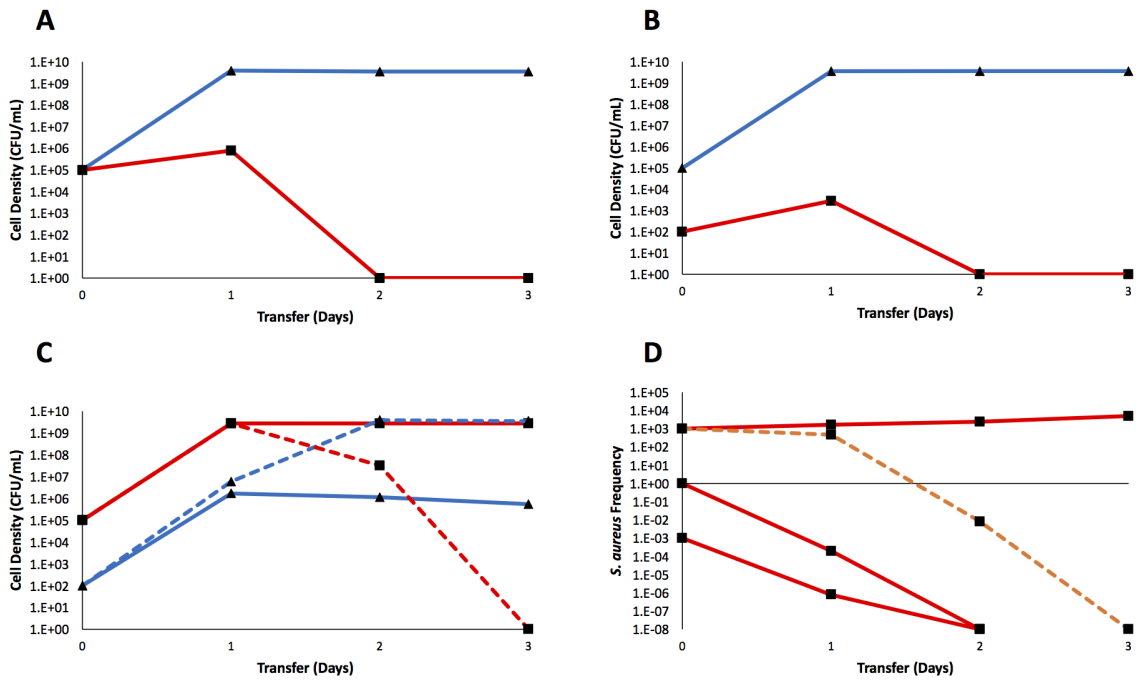

Figure 9: <u>A contact-dependent model with predation does not explain the observed dynamics when *P. aeruginosa* is initially rare</u> This is a simulation of the model outlined in Fig. 8A and Eq. 9-18. Parameters used are found in Tables 2 and 3. (Solid lines, $\delta = 1.75 \times 10^{-10}$; Dashed lines, $\delta = 4 \times 10^{-10}$.) While the experimental dynamics observed when *P. aeruginosa* is at equal initial frequency (A) and higher initial frequency (B) than *S. aureus* can be approximated by this model, those when *P. aeruginosa* is initially rare (C) are not well explained by this model. The kill rate constant, δ, must be increased to approximate the dynamics. Even with this enhanced killing accounted for when *P. aeruginosa* is initially rare, the frequency of *S. aureus* is higher than observed experimentally, after the first passage (D).

While the predation model can simulate the scenarios where *P. aeruginosa* is at equal or higher initial frequency to *S. aureus*, they fail to capture the dynamics observed when *P. aeruginosa* is rare (Fig. 9C). Using the same kill-rate constant (δ) as the equal and high frequency conditions, *P. aeruginosa* could not increase when rare (Fig. 9C, solid lines). To approximate the dynamics observed in Fig. 3E, δ was increased (Fig. 9C, dashed lines). In the simulated results with this increased kill rate constant, *P. aeruginosa* can increase in frequency when initially rare.

However, it is maintained at a density lower than *S. aureus* in the first passage, which is inconsistent with the experimental results shown in Fig. 3E.

For *P. aeruginosa* and *S. aureus* to reach the same density after one passage, with *P. aeruginosa* initially rare, the resource derived from *S. aureus* resource must be accessible before the killing occurs. One hypothesis is that *P. aeruginosa* can utilize free *N*-acetylglucosamine (GlcNAc) shed from the peptidoglycan found in the gram-positive cell wall of *S. aureus*. This phenomenon of *P. aeruginosa* using GlcNAc as a carbon source has already been observed by Korgaonkar and Whiteley, 2011. We add this observation to the models by changing the rate of appearance of the *S. aureus*-derived resource (R_{Sa}) to being only proportional to the density of living *S. aureus* (N_{Sa}), instead of proportional to the rate of *S. aureus* killing, as is the case in Fig. 8 (Fig. 10). If this phenomenon is added to either of the models shown in Fig. 1B and Fig. 1C, the observed *in vitro* dynamics when *P. aeruginosa* is either rare or at equal initial frequency are simulated. We refer to this theoretical framework as the "passively released *S. aureus* resource" model.

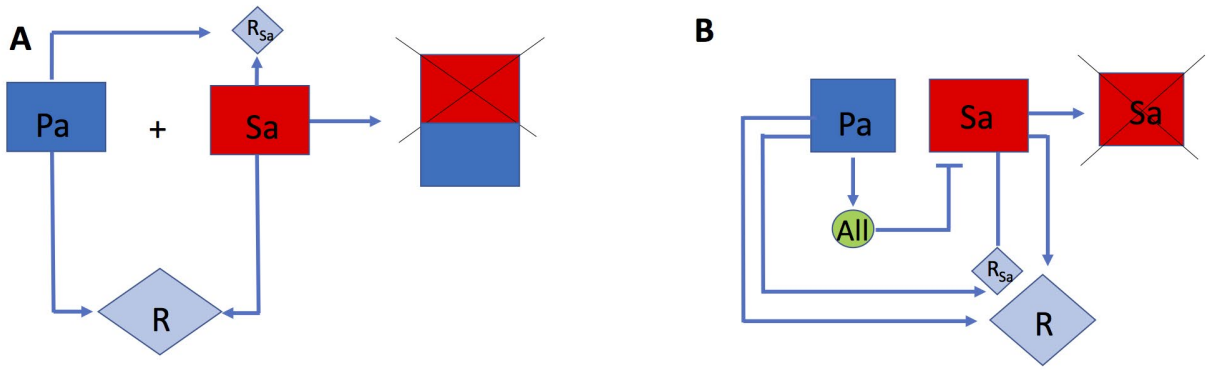

Figure 10: <u>Schematic diagrams of theoretical models, with a passively released *S. aureus*-derived resource</u> Direct contact-dependent (Eq. 25-29, A) and interspecies interaction-dependent extracellular allelopathy (Eq. 30-35, B) models, where *S. aureus* passively produces a resource that can be utilized by *P. aeruginosa*.

<u>Passively Released *S. aureus* Resource CDI Model (Eq. 25-29, Fig. 10A)</u>: Like the earlier models, *P. aeruginosa* and *S. aureus* interact through utilization of the shared resource (R). This model is an expanded version of the one shown in Fig. 1B, and described in Eq. 14-18, where *P. aeruginosa* kills *S. aureus* upon contact. This antagonistic interaction is modelled assuming mass

action, where the rate of killing is proportional to the product of the *P. aeruginosa* (N_{Pa}) and *S. aureus* (N_{Sa}) densities. This model differs from that in Fig. 1B and 8A because *S. aureus* is passively converted into a resource (R_{Sa}). The concentration of R_{Sa} is defined by the product of N_{Sa}, and the parameter, *l*. In addition to utilizing the common resource, *P. aeruginosa* can use R_{Sa} as a resource for growth at a rate proportional to a Monod function separate to that of the common resource ($\Psi(R_{Sa})$). With these definitions and assumption, as well as those of resource concentration-dependent growth, the rates of change in the densities of the bacterial populations and the concentration of the resource, in batch culture, are given by,

$$\frac{dR}{dt} = \underbrace{-\psi(R)\bullet(e_{Pa}\bullet v_{Pa}\bullet N_{Pa} + e_{Sa}\bullet v_{Sa}\bullet N_{Sa})}_{\text{Decline in Resource Concentration}} \tag{25}$$

$$\frac{dR_{Sa}}{dt} = \underbrace{l\bullet N_{Sa} - \psi\left(R_{Sa}\right)\bullet e_{Pa}\bullet v_{Pa}\bullet N_{Pa}}_{\substack{\text{Change in Concentration of the Resource} \\ \text{Derived From Lysis of } S.\,aureus \text{ Cells}}} \tag{26}$$

$$\frac{dN_{Pa}}{dt} = \underbrace{\left(\psi(R) + \psi(R_{Sa})\right)\bullet v_{Pa}\bullet N_{Pa}}_{\substack{\text{Increase in } P.\,aeruginosa \\ \text{Density}}} \tag{27}$$

$$\frac{dN_{Sa}}{dt} = \underbrace{\psi(R)\bullet v_{Sa}\bullet N_{Sa} - \delta\bullet N_{Pa}\bullet N_{Sa}}_{\substack{\text{Change in } S.\,aureus \text{ Density When} \\ \text{Inhibited by } P.\,aeruginosa, \text{ Upon Contact}}} \tag{28}$$

$$where\ \ \psi(R) = \frac{R}{(R+k)} \quad and \quad \psi(R_{Sa}) = \frac{R_{Sa}}{(R_{Sa}+k_{Sa})} \tag{29}$$

Passively Released *S. aureus* Resource Extracellular Allelopathy Model (Eq. 30-35, Fig. 10B): Like the earlier models, *P. aeruginosa* and *S. aureus* interact through utilization of the shared resource (R). This is an expanded version of the one shown in Fig. 1C, and described in Eq. 9-13, where *P. aeruginosa* produces an extracellular compound at a rate defined by the product of the of *P. aeruginosa* population density (N_{Pa}) and the parameter, β. This is modelled assuming mass action, where the rate of killing is proportional to the product of *P. aeruginosa* (N_{Pa}), *S. aureus* (N_{Sa}), and allelopathic agent (A) densities. This model differs from that in Fig. 1C and 8B because when the allelopathic agent kills *S. aureus*, *S. aureus* is passively converted into a resource (R_{Sa}). The concentration of R_{Sa} is defined by the product of N_{Sa}, and the parameter, *l*. In

addition to utilizing the common resource, *P. aeruginosa* can use R_{Sa} as a resource for growth at a rate proportional to a Monod function separate to that of the common resource ($\Psi(R_{Sa})$). With these definitions and assumption, as well as those of resource concentration-dependent growth, the rates of change in the densities of the bacterial populations and the concentration of the resource, in batch culture, are given by,

$$\frac{dR}{dt} = \underbrace{-\psi(R)\bullet(e_{Pa}\bullet v_{Pa}\bullet N_{Pa} + e_{Sa}\bullet v_{Sa}\bullet N_{Sa})}_{\text{Decline in Resource Concentration}} \tag{30}$$

$$\frac{dR_{Sa}}{dt} = \underbrace{l\bullet N_{Sa} - \psi\left(R_{Sa}\right)\bullet e_{Pa}\bullet v_{Pa}\bullet N_{Pa}}_{\substack{\text{Change in Concentration of the Resource} \\ \text{Derived From Lysis of } S.\text{aureus Cells}}} \tag{31}$$

$$\frac{dN_{Pa}}{dt} = \underbrace{\left(\psi(R)+\psi(R_{Sa})\right)\bullet v_{Pa}\bullet N_{Pa}}_{\text{Change in } P.\text{aeruginosa Density}} \tag{32}$$

$$\frac{dN_{Sa}}{dt} = \underbrace{\psi(R)\bullet v_{Sa}\bullet N_{Sa} - \gamma\bullet N_{Sa}\bullet A}_{\substack{\text{Change in } S.\text{aureus Density When} \\ \text{Inhibited by the Allelopathic Compound}}} \tag{33}$$

$$\frac{dA}{dt} = \underbrace{\left(\psi(R)+\psi(R_{Sa})\right)\bullet v_{Pa}\bullet\beta\bullet N_{Pa}}_{\substack{\text{Rate of Production of} \\ \text{the Allelopathic Compound}}} \tag{34}$$

$$\text{where } \psi(R) = \frac{R}{(R+k)} \quad \text{and} \quad \psi(R_{Sa}) = \frac{R_{Sa}}{(R_{Sa}+k_{Sa})} \tag{35}$$

If *P. aeruginosa* is at high initial frequency, *S. aureus* is lost more rapidly than observed experimentally in the passively released *S. aureus* resource models (simulated data not shown). It was observed in the simulations of the models shown in Fig. 10 that R_{Sa} reaches relatively high concentrations when *P. aeruginosa* is initially rare, and it is virtually zero when *P. aeruginosa* is initially equal or high in frequency, relative to *S. aureus*. The concentration of R_{Sa} is directly proportional to N_{Sa}. Korgaonkar and Whiteley, 2011, along with other studies, found that increased GlcNAc levels also lead to enhanced production of antimicrobial compounds in *P. aeruginosa* [21]. With the present study's *in silico* finding of increased R_{Sa} when *P. aeruginosa* is initially rare, coupled with the experimental observation of increased antimicrobial production with higher extracellular GlcNAc levels, we hypothesized that the coefficient of killing (δ for CDI or γ for extracellular allelopathy) increases with increasing R_{Sa} levels (Fig. 10B). We used *S. aureus* frequency as a proxy measurement for R_{Sa} levels, with higher frequencies of *S. aureus*

yielding more R_{Sa}. It should be noted that this change to the model is only meant to illustrate a concept. More thorough theoretical and experimental investigations need to be conducted to quantify any existing relationship between the hypothesized R_{Sa} and the rate of killing of *S. aureus* by *P. aeruginosa*. With these amendments, the simulated *S. aureus* density declines in a manner consistent with the *in vitro* experiments, when *P. aeruginosa* frequency is initially high. These results can be modelled for either extracellular allelopathy or CDI. A simulation of the representative CDI model is shown in Fig. 11. Notice the similarity in the population dynamics between this simulation and the *in vitro* results shown in Fig. 3.

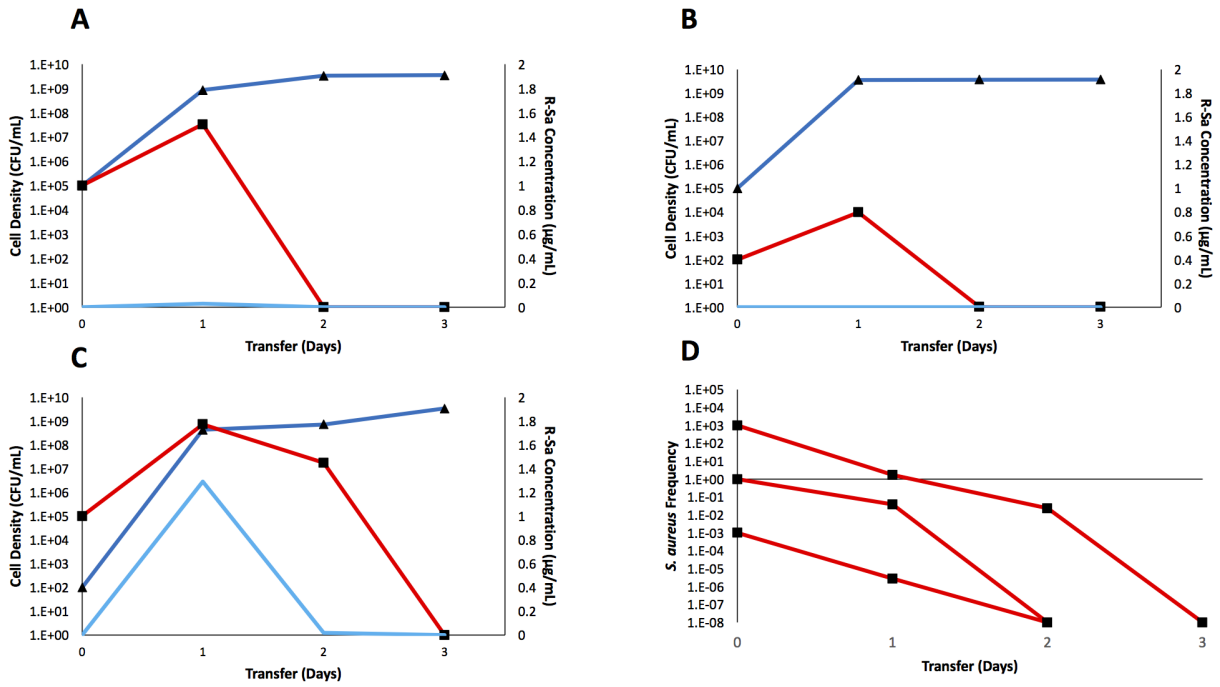

Figure 11: <u>A model where a product passively produced *S. aureus* induces *P. aeruginosa* antagonism and is used by *P. aeruginosa* as a resource simulates the results observed experimentally</u> Simulated results are shown for the model in Fig. 10A and Eq. 25-29. Parameters used are those found in Tables 3 and 4. The kill rate constant varies by panel, and increases with increasing frequency of *S. aureus* (Pa:Sa=1:1 (A): $\delta = 3.5 \times 10^{-10}$, Pa:Sa = 1:0.001 (B): $\delta = 1.5 \times 10^{-10}$; Pa:Sa = 0.001:1 (C): $\delta = 4.5 \times 10^{-10}$). *P. aeruginosa* (dark blue) has an advantage over *S. aureus* (red) at all initial frequencies. The resource derived from *S. aureus* (R-Sa, light blue) is most abundant when *P. aeruginosa* is initially rare. The frequency dependence of the interaction is summarized in D.

II. Population Dynamics and Antagonism in a Physically Structured Environment

Until this point, each of the *in vitro* experiments has been conducted in liquid media, where all exoproducts are evenly distributed throughout the mixture, and cells are free to move without any restriction. However, in nature, bacteria rarely exist under these theoretically convenient conditions. They oftentimes exist in biofilms, on two-dimensional surfaces, and three-dimensional matrices, all of which are likely present in the CF lung. In the next experiment, we add physical structure as a factor to the interaction. By doing so, different variables of the competition between *P. aeruginosa* and *S. aureus* can be examined. For this we use the surface slide system (SSS) developed by Lone Simonsen [22], where the bacteria exist and compete as colonies. This experimental system enables us to explore the effects of distance between colonies of *S. aureus* and *P. aeruginosa* on the nature and extent of the antagonism.

The SSS method: Pure overnight cultures of *P. aeruginosa* PAO1 WT (either with or without GFP) and *S. aureus* JE2 (either with or without Dsred) were prepared and sampled the next day, to measure initial cell densities. The overnight cultures were serially diluted in saline 1/10, 1/100, 1/1000, 1E-4, 1E-5, and 1E-6 to isolate initial cell populations (N_o) of approximately 1E7, 1E6, 1E5, 1E4, 1E2, respectively, in 25 µL aliquots. Autoclaved 3 inch by 1 inch glass microscope slides were obtained, and 1 mL of 1.5% LB hard agar was pipetted onto the slide. The LB agar surfaces were allowed to dry for 3-5 minutes. For the single-clone slides, 25 µL of the pure PAO1 WT and *S. aureus* JE2 cultures at the different dilutions were spread on top of the LB agar surfaces, using a glass spreader. Before and after each plate was prepared, the spreader was soaked in 100% ethanol and flamed. In the mixed culture slides, the dilutions were prepared by taking 50 µL from the previous PAO1 and *S. aureus* JE2 pure culture dilutions (e.g. to prepare $N_o \sim$ 1E5, draw from the $N_o \sim$ 1E6 dilution) and diluting this volume to obtain the desired initial cell population. These mixtures were then vortexed, and 25 µL of each dilution was spread on top of the LB agar surfaces, using the same methods as those implemented for the single-clone slides. The microscope slides were placed inside empty, plastic petri dishes. These dishes were stacked, placed in an air-tight metal cylinder, and incubated over night at 37˚ C.

The next day, slides were imaged at 4X magnification with no fluorescent filter, a GFP filter, and a Dsred filter using a Leica DMi8 S microscope. The agar surfaces were then suspended in 9 mL of saline, serially diluted, and sampled.

Initial Cell Population vs. Recovered Cell Density: Intercellular Distance Plays a Role in the Antagonism: In both PAO1 WT and SaJE2 single-clone culture slides, the agar surfaces were saturated at $N_o \sim$ 1E2 cells. In other words, the number of colonies was independent of the recovered cell density (CFU/mL), for the single-clone slides (Fig. 12A).

In the mixed culture slides, the populations of *S. aureus* are slightly lower when $N_o \sim$ 1E2 and $N_o \sim$ 1E4 cells than those of the single-clone slides for the same N_o values ($N_o \sim 1E2_{SINGLE(N=4)}$: 2E9 ± 5E8 CFU/mL, $N_o \sim 1E2_{MIX(N=3)}$: 4E8 ± 3E8 CFU/mL; $N_o \sim 1E4_{SINGLE(N=4)}$: 5E9 ± 2E9 CFU/mL, $N_o \sim 1E4_{MIX(N=4)}$: 7E8 ± 1E8 CFU/mL). However, the recovered *S. aureus* density more precipitously declines once N_o reaches ~1E5 cells ($N_o \sim 1E5_{SINGLE(N=3)}$: 4E9 ± 2E9 CFU/mL; $N_o \sim 1E5_{MIX(N=3)}$: 1E7 ± 2E7 CFU/mL) (Fig. 12B). The difference in recovered density between the single-clone and mixed slides is statistically significant when $N_o \sim$ 1E7 cells ($N_o \sim 1E7_{SINGLE(N=4)}$: 5E9 ± 2E9 CFU/mL; $N_o \sim 1E7_{MIX(N=4)}$: 2E4 ± 2E7 CFU/mL; two sample, unpaired t-test, assuming unequal variance: $p<0.05$).

Visualizing the Competition: A Revision of the Bacteriocin Model: For the single-clone slides, individual colonies of PAO1 WT (GFP) and *S. aureus* JE2 (Dsred) colonies are prevalent for initial cell populations less than $N_o \sim$ 1E5 for *P. aeruginosa*. Individual *S. aureus* colonies are visible at all initial cell populations. For $N_o \geq$1E5 in *P. aeruginosa*, cells cease organization into colonies and begin adopting a uniform lawn distribution. This could be due to a change in *P. aeruginosa* physiology as cells are closer together in the log phase of growth.

In the mixed culture microscopy images, colonies of PAO1 WT (GFP) and *S. aureus* JE2 (Dsred) grow in the same vicinity, which is inconsistent with the notion of *P. aeruginosa* secreting an extracellular compound that inhibits *S. aureus*. There is also qualitative increase in green fluorescence (*P. aeruginosa* density) in the regions immediately surrounding *S. aureus* colonies. This observation is consistent with the hypothesis that *S. aureus* passively sheds

GlcNAc (or some other compound) that *P. aeruginosa* can use as a resource. There is evidence of *S. aureus* colony growth for all N_o values, in the mixed culture slides, even though there are reductions in recovered densities on the plates (Fig. 12C).

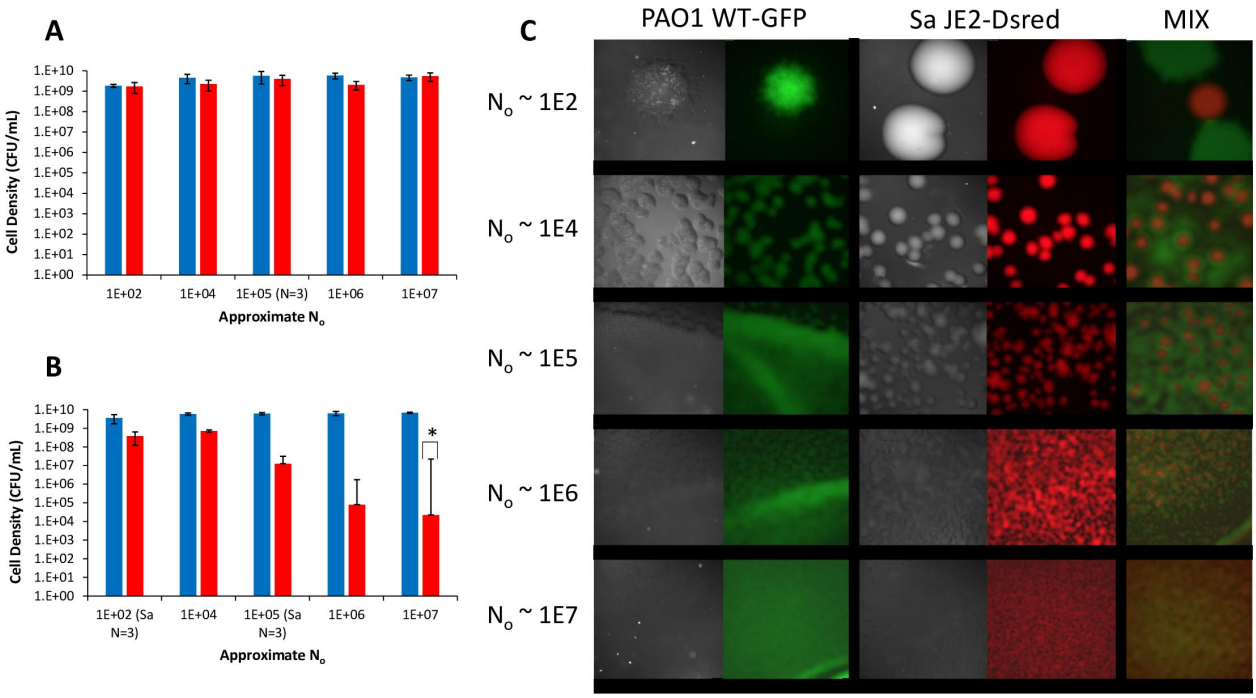

Figure 12: *P. aeruginosa* antagonism towards *S. aureus* occurs in a density dependent manner and requires a short *P. aeruginosa-S.aureus* intercellular distance. *P. aeruginosa* and *S. aureus* colonies can grow in the same vicinity, with *S. aureus* visible even with initial populations (N_o) ~1E7 cells Different initial populations of PAO1 WT (blue bars) and *S. aureus* JE2 (red bars) were spread onto two-dimensional agar surfaces. The mean recovered density, after one night of incubation, for four independent experiments is shown unless otherwise specified. Error bars represent the S.E.M. In the single-clone slides, N_o is independent of the recovered density after incubation for both *P. aeruginosa* and *S. aureus* (A). In the mixed population slides, *S. aureus* density begins to decline at N_o ~ 1E5 cells, and this reduction in recovered density increases with larger N_o values (B). Statistically significant differences between the mixed culture slide recovered density and the single-clone culture slides are marked with asterisks (*, $p<0.05$; **, $p<0.01$; ***, $p<0.001$). Representative slides were imaged using phase contrast microscopy, with PAO1 marked with GFP and *S. aureus* JE2 marked with Dsred (C). The first two panels are images

single-clone slides (left=without fluorescence, right=with fluorescence), and the third panel is a mixed culture slide with fluorescence (C). The mixed culture image was generated by overlaying the same image with GFP and Dsred filters.

DISCUSSION

This study set out characterize the population dynamics of the competitive interaction between *P. aeruginosa* and *S. aureus*. Understanding this ecology is not only of academic interest: These two normally commensal microbes are among the most common invaders of the CF lung [2]. Therefore, understanding how these species behave at the population level will inevitably lead to a better understanding of polymicrobial infections, both in the CF lung and in general. It has for a long time been known that *P. aeruginosa* either inhibits the growth of, or kills, *S. aureus*, both *in vitro* and *in vitro* [6, 7, 12, 23] . As technology has advanced, it has become easier to characterize the molecular and genetic basis of this interaction. Recent studies have shown that an interplay between the *P. aeruginosa* PQS quorum sensing system, particularly the molecule HQNO, and iron scavenging pathways involving the siderophores pyoverdine and pyocyancin [2, 6, 7, 13, 17, 23-25]. Despite the knowledge of this antagonism's existence and what has been discovered regarding *the P. aeruginosa* genetic mechanism, very little is known about how these bacteria interact at the population level. This study aimed to answer four questions regarding the population dynamics and evolution of *P. aeruginosa* antagonism towards *S. aureus* using a combination of mathematical simulations and *in vitro* experiments, both in liquid culture and on two-dimensional surfaces.

The first question asked if there were factors besides HQNO, specifically at the population level, that contribute to the antagonism. With competition between different types of bacteria, or any species, it is necessary to determine if the primary driving force for the observed population dynamics is competition for a limiting resource (i.e. the null model). If all other factors are equal, the bacterium with the faster growth rate and shorter lag time is expected to predominate in the long-run, while the strain that grows more slowly is eventually eradicated from the population. Based on short-term growth data, we found no appreciable difference in the growth rates of *P. aeruginosa* and *S. aureus,* and we demonstrated that *S. aureus* has a shorter lag time than *P.*

aeruginosa. If the null model were true, over time, *S. aureus* should beat *P. aeruginosa*. Since this dynamic is not observed, it is evident that there is an additional mechanism that leads to the antagonism. Based on the literature regarding HQNO and siderophores, we hypothesized that *P. aeruginosa* secretes molecules that inhibit, or kill, *S. aureus*, via an extracellular allelopathy mechanism. However, the mechanism where *P. aeruginosa* kills *S. aureus* upon direct contact (CDI) yields very similar results, so this process cannot be ruled out based solely upon data from mathematical modelling and competition experiments. Contact-based toxin mechanisms have already been observed in *P. aeruginosa*, which often employs a Type VI secretion system (T6SS) [26]. Similar mechanisms have also been demonstrated in *E. coli* and *C. crescentus* [19, 20].

In attempt to ascertain whether the interaction was driven solely by the density of *P. aeruginosa*, or by an interaction between *P. aeruginosa* and *S. aureus*, we conducted experiments using sonicated cell-free extracts of *P. aeruginosa.* We asked if this supernatant can exhibit the same degree of inhibition as *P. aeruginosa* living cells and if *P. aeruginosa* supernatant gave *S. aureus* a growth disadvantage. If the supernatant exhibited equal inhibitory qualities to the living cells, then this would serve as evidence that allelopathy, independent upon interspecies interactions, exclusively drives the observed antagonism. We found that the presence of sonicated *P. aeruginosa* supernatant had no effect on the recovered density of *S. aureus* cells, but it did cause a decreased growth rate and an increased lag time in *S. aureus*. In the same short-term growth experiment, the sonicated supernatant of the PAO1 *pqsL* mutant, which does not produce HQNO, only led to an increase in lag time. Taken together, these observations serve as evidence that HQNO plays some role in the antagonistic interaction, but that molecule alone does not entirely explain the mechanism, especially with respect to *S. aureus* cell lysis. Further, these experiments alone do not address whether HQNO, and other possible inhibitory molecules, are secreted or delivered to *S. aureus* cells upon contact, since sonication breaks cells open.

To determine if the inhibition requires living *P. aeruginosa* cells, we cultured *S. aureus* in the presence of non-replicating *P. aeruginosa* and found evidence that *S. aureus* was being killed by the stationary *P. aeruginosa*. This reduction in density is consistent with the notion of *P. aeruginosa* lysing *S. aureus*. Since the same cultures with the cells removed failed to kill *S. aureus*, these observations serve as evidence that the antagonism is due to a cross-species

interaction between living cells. This proposed cell-cell interaction can either take the form of CDI or *S. aureus* inducing of the production and/or secretion of the allelopathic agent.

Regardless of whether the mechanism is extracellular or contact-dependent, similar population dynamics to those observed in bacteriocins are expected. Bacteriocins, which are small toxic proteins produced by some strains of *E. coli*, operate via a simple extracellular allelopathy mechanism: When grown in liquid culture, cells that produce the toxic compound can only increase in frequency if they are at high or equal initial frequency in the population, relative to sensitive cells. If the antagonistic species is rare, it cannot overtake the population [27]. To determine if *P. aeruginosa* and *S. aureus* behave in a similar manner, mixed cultures of each species, started at different initial frequencies, were serially passaged. Contrary to what was observed with the bacteriocins, *P. aeruginosa,* the hypothesized “producer", always predominated, even when initially rare in the population. This finding demonstrates that the *P. aeruginosa*-*S. aureus* interaction cannot be explained by a simple extracellular allelopathy or CDI model.

Therefore, for *P. aeruginosa* to have an advantage when rare, we hypothesized that there must exist additional components to the mechanism of the antagonism independent of the intercellular killing mechanism itself. The second question this study aimed to answer pertained to how much of the observed population dynamics were due to antagonistic mechanisms. In the literature, competition for resources, especially iron, has been hypothesized as a major reason for *P. aeruginosa* antagonism towards *S. aureus*. Mashburn et al., 2005 found that *P. aeruginosa* lyses *S. aureus* to use it as an iron source. We began by incorporating this observation into the mathematical models. Based on the simulations with this expansion, initially rare *P. aeruginosa* can increase in frequency, and eventually overtake the population. However, we had to increase the kill rate constant to observe the *P. aeruginosa* population ascendance, when initially rare. This change could either reflect either a shortcoming of the model or that the rate of killing is, by some mechanism, higher when *P. aeruginosa* is initially rare. Even with this parameter at an increased value, the manner by which *P. aeruginosa* kills *S. aureus* in the *in vitro* serial passage experiments was markedly different than what was observed in the simulated results. In the simulations, *P. aeruginosa* grew to a density lower than *S. aureus* in the first passage, reaches the same density in the second passage, and then *S. aureus* was eradicated by the third passage. In

the experimental results, *P. aeruginosa* was at the same density as *S. aureus* for the first two passages and was eradicated during the third.

To capture these dynamics theoretically, we hypothesized that *S. aureus* passively releases a compound that can be used as a resource for *P. aeruginosa*. This is consistent with previous observations that *P. aeruginosa* can grow using peptidoglycan-derived GlcNAc as a carbon source and that GlcNAc can increase the production of *P. aeruginosa* antimicrobial compounds, including those associated with the PQS system [25, 28]. Additionally, it has been shown that peptidoglycan-derived GlcNAc can increase *P. aeruginosa* antagonism towards *S. aureus* and other gram-positive bacteria [21]. With this addition to the models, the experimental population dynamics can be simulated for both the extracellular allelopathy and CDI mechanisms.

In spite of these findings, it is still unclear at this point as to whether the mechanism is extracellular or requires cell-cell contact, which was the third question the present study aimed to answer. As a further experiment to help answer this question, we examined the growth of *P. aeruginosa* and *S. aureus* on two-dimensional surfaces, using the SSS method [22]. This method is also more consistent with how bacterial populations present in nature, as they are rarely found in well-mixed, sufficiently nourished, liquid environments. Prepared using the SSS protocol, single-clone cultures of *P. aeruginosa* and *S. aureus* grow to the same final density, regardless of the initial number of cells plated. In spite of these equivalent recovered densities, as *P. aeruginosa* initial cell population increased, the morphology of the cells, after one night of culturing, changed from mostly colonies to a uniform lawn. This phenomenon was not as pronounced, if at all present, in *S. aureus*. This change in *P. aeruginosa* morphology could be due to a difference in cell physiology when cells are closer together during the log phase of the growth cycle. Since the *S. aureus* density declines at the same time this change in *P. aeruginosa* morphology occurs, there may also be an increase in the antagonistic behavior of *P. aeruginosa* associated with this lawn morphology.

The microscopy images obtained in this study are inconsistent with those from Chao and Levin, 1981. That study found zones of clearance surrounding toxin-producing colonies, in soft agar matrices. No such zones were observed presently: *P. aeruginosa* and *S. aureus* grow in the same vicinity, with an apparent increase in *P. aeruginosa* density in the regions immediately surrounding *S. aureus* colonies. This observation is consistent with the passive *S. aureus*

resource model: Since GlcNAc density is likely highest in the region closest to the *S. aureus* colonies, *P. aeruginosa* can grow to a higher density and produce toxins at a higher rate in this area (Fig. 13). In the context of this phenomenon, one could then hypothesize that there is increased killing of *S. aureus* by these more proximal *P. aeruginosa* cells. While these experiments demonstrated density dependence and population interactions in two-dimensions, it is still unclear as to whether the mechanism is extracellular or contact-dependent, as both could potentially explain the SSS dynamics using the *S. aureus*-derived resource model. Completely addressing the contact-dependence question will likely require a flow cytometry study, as has been implemented in other studies that have demonstrated the existence of CDI [19, 20].

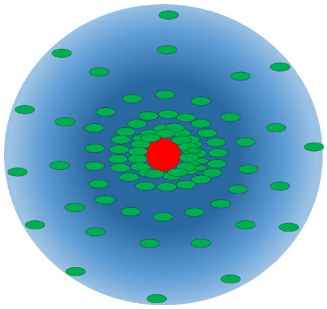

Figure 13: <u>Possible Model that explains SSS Observations</u> A compound (blue), perhaps GlcNAc, is passively released by *S. aureus* and forms a gradient surrounding the *S. aureus* colony (red circle). *P. aeruginosa* (green rods) can grow on this compound, and as a result, can reach higher densities closer to the *S. aureus* colony, where the compound density is highest. *P. aeruginosa* cells that are closest to the *S. aureus* colony not only receive the highest amounts of the *S. aureus*-derived compound, but are also induced to be the most antagonistic towards *S. aureus*.

One of the major limitations of the present study is that while it characterizes the population dynamics of the interaction, it does not fully address the evolution and maintenance of the antagonism. Based on the rare *P. aeruginosa* advantage, and the simulated dynamics of the expanded *S. aureus*-derived resource models, we hypothesize that *P. aeruginosa* antagonism towards *S. aureus* evolved as a mechanism to obtain additional resources from *S. aureus*. This finding is consistent with Mashburn et al., 2005 and Koronkar and Whiteley, 2011.

For experimental verification of the resource-based hypotheses put forth in this study, future research should look to the literature devoted to the evolution of antagonism in bacteriocin systems. While we have shown that the *P. aeruginosa*-*S. aureus* system is distinct from the canonical bacteriocin model, it can still be used as a starting point for understanding its evolution. Based on the experiments conducted to understand the evolution of bacteriocin systems, it can be hypothesized that extracellular allelopathy should confer no advantage to *P. aeruginosa* in liquid culture, whereas it should cause an advantage in a structured growth environment. In liquid culture, the allelopathic agent can freely diffuse in the media, and both *P. aeruginosa* strains can benefit equally from its presence. In other words, the non-producing strain would be acting as a cheater [27, 29]. The present study found that the producer *P. aeruginosa* (PAO1 WT) has a fitness disadvantage relative to the cheater (PAO1 *pqsL*), so the non-producer would be expected to increase in frequency over time, if both strains were mixed together with *S. aureus*. If the mechanism were contact-dependent, the dynamic would change since producers would have an advantage not shared with cheaters. However, since the hypothesized cheater strain used in the present study has a growth advantage relative to the WT strain, one would need to observe if the growth rate advantage from not producing the toxin outweighs the resource acquisition advantage from killing *S. aureus.*

The dynamic of bacteriocin systems changes in physically structured environments. In Chao and Levin, 1981, toxic *E. coli* had a disadvantage due to the fitness cost of toxin production in liquid media, but nevertheless increased in frequency when cultured in soft agar. The interpretation of this result is that the more toxic strain killed surrounding toxin-sensitive bacteria, thereby increasing the producer's relative share of the resource. Extension of this theoretical interpretation to the present system is complicated by the fact that we have shown evidence that the presence of *S. aureus* may constitute as a resource for *P. aeruginosa*, so clearing *S. aureus* from its vicinity may not be necessarily advantageous.

The *P. aeruginosa*-*S. aureus* antagonistic relationship can also be examined through the framework of the "rock-paper-scissors" (RPS) model of allelopathy by Kerr et al., 2002. In the RPS model, there are three strains of bacteria: a toxin producer, a cheater that produces less of the toxin, and a toxin-sensitive population. The RPS model already assumes that cheaters have a growth advantage over producers, consistent with what was observed in the present study [30].

This adaptation leads to cheater ascendance in liquid cultures, with eventual extinction of the producer [30]. When these same strains are cultured in resource-partitioned, structured environments, all strains co-exist [30]. Replication of these results with *P. aeruginosa* and *S. aureus* would support an extracellular allelopathy mechanism.

CF polymicrobial infections can be considered an extension of the evolution and population dynamics of bacterial interactions. Based on the natural history of CF infections, *P. aeruginosa* colonizes the lungs of these patients after an *S. aureus* infection has already been established [1-4]. In other words, *P. aeruginosa* is initially rare in these infections, yet it regularly co-infects with *S. aureus* and oftentimes outcompetes it. From the results of this study, and the passive *S. aureus* resource model, we hypothesize that *P. aeruginosa* uses GlcNAc, or other *S. aureus* exoproducts, as resources to grow, facilitate niche establishment, and eventually overtake *S. aureus* populations in CF infections. Based on the SSS data, we hypothesize that the presentation of co-infection could be due to a physical distance between cells of the two species within the lungs of these patients. In chronic wound infections, it has been observed that *P. aeruginosa* and *S. aureus* adopt a non-random spatial arrangement, with *S. aureus* occupying more superficial regions of the wound and *P. aeruginosa* colonizing deeper portions [31]. Similarly, spatial distributions that keep populations of each species distant could be occurring within the lungs of CF patients, but the difficulty of observing how each species occupies the lungs *in vivo* complicates direct observation of this possible phenomenon. Other studies have cited the mucoid phenotype of *P. aeruginosa* as being less antagonistic towards *S. aureus* and small colony variant *S. aureus* as being refractory to *P. aeruginosa* inhibition as reasons for the existence of these co-infections [2, 8, 10, 32-34]. These previous findings, based on phenotypic variation within each species, are not mutually exclusive with the findings of this study, which are based upon population dynamics and physical structure. Mass action models, like those used in the present study, are insufficient to theoretically model the dynamics of competition influenced by physical structure. Partial differential equation models have been used to model bacterial colony growth and the dynamics observed in physically structured bacteriocin systems [33, 34]. Models such as these could feasibly be extended to characterize the competition of colonies from different species in the SSS method and the population dynamics of the interaction in three-dimensional spaces. Providing a theoretical framework to understand the population dynamics of bacteria in

physical structures will likely lead to the development of more effective treatments and models of antibiotic resistance.

REFERENCES

1. Lyczak, J.B., C.L. Cannon, and G.B. Pier, *Lung infections associated with cystic fibrosis.* Clin Microbiol Rev, 2002. **15**(2): p. 194-222.
2. Filkins, L.M., et al., *Coculture of Staphylococcus aureus with Pseudomonas aeruginosa Drives S. aureus towards Fermentative Metabolism and Reduced Viability in a Cystic Fibrosis Model.* J Bacteriol, 2015. **197**(14): p. 2252-64.
3. Harrison, F., *Microbial ecology of the cystic fibrosis lung.* Microbiology, 2007. **153**(Pt 4): p. 917-923.
4. Rajan, S. and L. Saiman, *Pulmonary infections in patients with cystic fibrosis.* Semin Respir Infect, 2002. **17**(1): p. 47-56.
5. Limoli, D.H., et al., *Staphylococcus aureus and Pseudomonas aeruginosa co-infection is associated with cystic fibrosis-related diabetes and poor clinical outcomes.* Eur J Clin Microbiol Infect Dis, 2016. **35**(6): p. 947-53.
6. Nguyen, A.T. and A.G. Oglesby-Sherrouse, *Interactions between Pseudomonas aeruginosa and Staphylococcus aureus during co-cultivations and polymicrobial infections.* Appl Microbiol Biotechnol, 2016. **100**(14): p. 6141-8.
7. Machan, Z.A., et al., *2-Heptyl-4-hydroxyquinoline N-oxide, an antistaphylococcal agent produced by Pseudomonas aeruginosa.* J Antimicrob Chemother, 1992. **30**(5): p. 615-23.
8. Hoffman, L.R., et al., *Selection for Staphylococcus aureus small-colony variants due to growth in the presence of Pseudomonas aeruginosa.* Proc Natl Acad Sci U S A, 2006. **103**(52): p. 19890-5.
9. Schertzer, J.W., M.L. Boulette, and M. Whiteley, *More than a signal: non-signaling properties of quorum sensing molecules.* Trends Microbiol, 2009. **17**(5): p. 189-95.
10. McNamara, P.J. and R.A. Proctor, *Staphylococcus aureus small colony variants, electron transport and persistent infections.* Int J Antimicrob Agents, 2000. **14**(2): p. 117-22.
11. Mashburn, L.M., et al., *Staphylococcus aureus serves as an iron source for Pseudomonas aeruginosa during in vivo coculture.* J Bacteriol, 2005. **187**(2): p. 554-66.
12. Palmer, K.L., et al., *Cystic fibrosis sputum supports growth and cues key aspects of Pseudomonas aeruginosa physiology.* J Bacteriol, 2005. **187**(15): p. 5267-77.
13. Diggle, S.P., et al., *The Pseudomonas aeruginosa 4-quinolone signal molecules HHQ and PQS play multifunctional roles in quorum sensing and iron entrapment.* Chem Biol, 2007. **14**(1): p. 87-96.
14. Nguyen, A.T., et al., *Iron Depletion Enhances Production of Antimicrobials by Pseudomonas aeruginosa.* J Bacteriol, 2015. **197**(14): p. 2265-75.
15. Limoli, D.H., et al., *Interspecies interactions induce exploratory motility in Pseudomonas aeruginosa.* Elife, 2019. **8**.
16. Fey, P.D., et al., *A genetic resource for rapid and comprehensive phenotype screening of nonessential Staphylococcus aureus genes.* mBio, 2013. **4**(1): p. e00537-12.
17. Lin, J., et al., *The Pseudomonas Quinolone Signal (PQS): Not Just for Quorum Sensing Anymore.* Front Cell Infect Microbiol, 2018. **8**: p. 230.
18. Stewart, F.M. and B.R. Levin, *Partitioning of Resources and the Outcome of Interspecific Competition: A Model and Some General Considerations.* The American Naturalist, 1973. **107**(954): p. 171-198.
19. Lemonnier, M., et al., *The evolution of contact-dependent inhibition in non-growing populations of Escherichia coli.* Proc Biol Sci, 2008. **275**(1630): p. 3-10.
20. Garcia-Bayona, L., M.S. Guo, and M.T. Laub, *Contact-dependent killing by Caulobacter crescentus via cell surface-associated, glycine zipper proteins.* Elife, 2017. **6**.
21. Korgaonkar, A., et al., *Community surveillance enhances Pseudomonas aeruginosa virulence during polymicrobial infection.* Proc Natl Acad Sci U S A, 2013. **110**(3): p. 1059-64.
22. Simonsen, L., *Dynamics of plasmid transfer on surfaces.* J Gen Microbiol, 1990. **136**(6): p. 1001-7.
23. Machan, Z.A., et al., *Interaction between Pseudomonas aeruginosa and Staphylococcus aureus: description of an anti-staphylococcal substance.* J Med Microbiol, 1991. **34**(4): p. 213-7.

24. Haussler, S. and T. Becker, *The pseudomonas quinolone signal (PQS) balances life and death in Pseudomonas aeruginosa populations.* PLoS Pathog, 2008. **4**(9): p. e1000166.
25. Hotterbeekx, A., et al., *In vivo and In vitro Interactions between Pseudomonas aeruginosa and Staphylococcus spp.* Front Cell Infect Microbiol, 2017. **7**: p. 106.
26. Wood, T.E., et al., *The Pseudomonas aeruginosa T6SS Delivers a Periplasmic Toxin that Disrupts Bacterial Cell Morphology.* Cell Rep, 2019. **29**(1): p. 187-201 e7.
27. Chao, L. and B.R. Levin, *Structured habitats and the evolution of anticompetitor toxins in bacteria.* Proc Natl Acad Sci U S A, 1981. **78**(10): p. 6324-8.
28. Korgaonkar, A.K. and M. Whiteley, *Pseudomonas aeruginosa enhances production of an antimicrobial in response to N-acetylglucosamine and peptidoglycan.* J Bacteriol, 2011. **193**(4): p. 909-17.
29. Travisano, M. and G.J. Velicer, *Strategies of microbial cheater control.* Trends Microbiol, 2004. **12**(2): p. 72-8.
30. Kerr, B., et al., *Local dispersal promotes biodiversity in a real-life game of rock-paper-scissors.* Nature, 2002. **418**(6894): p. 171-4.
31. Fazli, M., et al., *Nonrandom distribution of Pseudomonas aeruginosa and Staphylococcus aureus in chronic wounds.* J Clin Microbiol, 2009. **47**(12): p. 4084-9.
32. Limoli, D.H., et al., *Pseudomonas aeruginosa Alginate Overproduction Promotes Coexistence with Staphylococcus aureus in a Model of Cystic Fibrosis Respiratory Infection.* mBio, 2017. **8**(2).
33. Shao, X., et al., *Growth of bacteria in 3-d colonies.* PLoS Comput Biol, 2017. **13**(7): p. e1005679.
34. Durrett, R. and S. Levin, *Allelopathy in Spatially Distributed Populations.* J Theor Biol, 1997. **185**(2): p. 165-71.